

Review of Canadian Aeronautical Fatigue and Structural Integrity Work 2013-2015

Authors: Nicholas C. Bellinger

Report No.: LTR-SMM-2015-0002

RDIMS No.: N/A

Date: April 2015

NATIONAL RESEARCH COUNCIL CANADA

AEROSPACE

Review of Canadian Aeronautical Fatigue and Structural Integrity Work 2013-2015

Volume 1 of 1

Report No.: LTR-SMM-2015-0002

RDIMS No.: N/A

Date: April 2015

Authors: Nicholas C. Bellinger

Classification:	Unclassified	Distribution:	Unlimited
For:	International Committee on Aeronautical Fatigue and Structural Integrity (ICAF)		
Reference:	-		
Submitted by:	S. Béland, Director, Structures, Materials and Manufacturing Laboratory		
Approved by:	J. Komorowski, General Manager, Aerospace Portfolio		

Pages :	76	Copy No.:	N/A
Figures:	65	Tables:	3

This Report May Not Be Published Wholly Or In Part Without The Written Consent Of The National Research Council Canada

EXECUTIVE SUMMARY

This report provides a review of Canadian work associated with aeronautical fatigue and structural integrity during the period 2013 – 2015. All aspects of structural technology are covered including full-scale tests, loads monitoring, fracture mechanics, composite materials and non-destructive inspection.

Organization abbreviations used in this document are:

BA – Bombardier Aerospace

BHTC – Bell Helicopter Textron Canada

RCAF – Royal Canadian Air Force (CF)

DRDC – Defence Research and Development Canada (DND)

DND – Department of National Defence

DTAES – Directorate of Technical Airworthiness and Engineering Support (DND)

L-3 MAS – L-3 Communications (Canada) Military Aircraft Services (MAS)

NRC – National Research Council Canada

RMC – Royal Military College of Canada (DND)

TABLE OF CONTENTS

EXECUTIVE SUMMARY	I
TABLE OF CONTENTS	II
ABBREVIATIONS.....	IV
1.0 INTRODUCTION.....	1
2.0 FULL-SCALE AND COMPONENT TESTING.....	2
2.1 CF-18 FLIGHT CONTROL SURFACES LIFE EXTENSION	2
2.2 OUTER WING CERTIFICATION	3
2.3 F/A-18 FT905 CF-18 HORIZONTAL STABILATOR FATIGUE TEST	3
2.4 DASH-8 MODEL 100 ESP SUMMARY	5
2.5 CSERIES DURABILITY AND DAMAGE TOLERANCE TESTS	6
3.0 PROBABLISTIC AND RISK ANALYSIS METHODS.....	11
3.1 INTEGRATED STRUCTURAL LIFE ASSESSMENT TECHNOLOGIES FOR ROYAL CANADIAN AIR FORCE FLEETS*.....	11
3.1.1 <i>References</i>	13
3.2 DEVELOPMENT OF IMPROVED METHODOLOGIES FOR MULTIPLE SITE DAMAGE TOLERANCE ANALYSIS	16
3.2.1 <i>References</i>	17
3.3 DEVELOPMENT OF AN IN-SERVICE DAMAGE ASSESSMENT TOOL	17
3.3.1 <i>References</i>	17
3.4 FATIGUE LIFE IMPROVEMENT FACTOR OF COLD WORKED HOLES FOR THE CP-140/P-3 OUTER WING ASSEMBLY.....	18
3.4.1 <i>Reference</i>	19
4.0 STRUCTURAL INTEGRITY	20
4.1 CT114 (TUTOR) AIRCRAFT STRUCTURAL INTEGRITY PROGRAM (ASIP)	20
4.2 S-92 MARITIME HELICOPTER (CYCLONE)	21
4.3 CF-18 AIRCRAFT STRUCTURAL INTEGRITY PROGRAM (ASIP) AND LIFE EXTENSION PROGRAM (ALEX).....	21
4.4 F-18 INTERNATIONAL SUPPORT	23
4.5 MULTI-PURPOSE ATMOSPHERIC PLASMA FOR PAINT STRIPPING AND ENHANCED LPI	24
4.5.1 <i>References</i>	25
4.6 SAFETY CUTS IN FATIGUE DAMAGED FASTENER HOLES	26
4.7 FATIGUE PERFORMANCE CHARACTERIZATION OF A COMPOSITE BUTT JOINT CONFIGURATION	27
4.7.1 <i>Reference</i>	29
4.8 MODELING OF PROGRESSIVE FAILURE IN BONDED COMPOSITE JOINT	29
4.8.1 <i>References</i>	32
4.9 LONG-TERM DURABILITY OF ADHESIVELY BONDED COMPOSITE JOINTS UNDER STATIC AND FATIGUE LOADING*	32
5.0 FRACTURE MECHANICS AND CRACK PROPAGATION STUDIES.....	35
5.1 A MECHANISM-BASED APPROACH TO CREEP, LOW CYCLE FATIGUE AND THERMOMECHANICAL FATIGUE LIFE PREDICTION.....	35
5.1.1 <i>References</i>	36
5.2 APPLICATION OF EXPERIMENTAL MECHANICS TECHNIQUES FOR BIAXIAL FATIGUE TESTING.....	36

Review of Canadian Aeronautical Fatigue and Structural Integrity Work 2013-2015

5.3	QUANTITATIVE FATIGUE DAMAGE MEASUREMENTS IN CARBON FIBRE REINFORCED POLYMERS.....	37
5.3.1	References.....	40
5.4	TENSILE FATIGUE BEHAVIOUR OF TAPERED GLASS FIBRE REINFORCED EPOXY COMPOSITES CONTAINING NANOCCLAY	40
5.5	BENCHMARK ASSESSMENT ON FATIGUE PROPAGATION IN A BONDED COMPOSITE JOINT STRUCTURE.....	42
5.5.1	References.....	44
5.6	NUMERICAL PREDICTIONS OF EVOLVING CRACK FRONT GEOMETRY AND FATIGUE LIFE FROM STRAIGHT AND COUNTERSUNK HOLES IN THIN PLATES	44
5.6.1	References.....	46
5.7	DEVELOPMENT OF A FATIGUE CRACK GROWTH RATE MATERIAL MODEL FOR 7249-T76511 ALUMINIUM ALLOY*.....	46
5.8	PREDICTIVE MODELING FOR FOUR-POINT BENDING OF THIN CARBON-EPOXY LAMINATES.....	49
6.0	USAGE AND STRUCTURAL HEALTH MONITORING.....	51
6.1	DATA REDUCTION OF FLIGHT TEST AND FEM DATA SETS AND APPLICATION TO FATIGUE LOAD SPECTRA DEVELOPMENT	51
6.2	ENVIRONMENTAL CONDITIONING FOR STRUCTURAL HEALTH MONITORING SYSTEM RELIABILITY*	53
6.3	LOW COST ACOUSTIC EMISSION SYSTEM FOR CRACK DETECTION IN STRUCTURAL HEALTH MONITORING TEST PLATFORM.....	54
6.4	KRACK INDICATOR SENSOR (KIS) TECHNOLOGY DEVELOPMENT – STRUCTURAL CRACK DETECTION & MONITORING	55
6.5	HELICOPTER LOAD AND USAGE MONITORING: RESEARCH ACTIVITIES 2013-2015.....	58
7.0	NON-DESTRUCTIVE EVALUATION.....	61
7.1	DEVELOPMENT OF INDUCTION HEATING THERMOGRAPHY	61
7.2	DEVELOPMENT OF MODELLING CAPABILITIES FOR INDUCTION HEATING THERMOGRAPHY	61
7.3	COMPARATIVE ASSESSMENT OF NDT FOR THE INSPECTION OF CF18 OUTBOARD FORWARD RIB	62
7.4	ASSESSMENT OF SHEAROGRAPHY FOR NDI OF COMPOSITE MATERIAL	63
7.5	MODEL-ASSISTED PROBABILITY OF DETECTION ASSESSMENT FOR ENGINE COMPONENTS	64

ABBREVIATIONS

ACR	Adjusted Compliance Ratio
ACGR	Automatic Crack Growth Program
AE	Acoustic Emission
ALEX	Aircraft Life Extension Program
ASI	Aircraft Sampling Inspections
ASIP	Aircraft Structural Integrity Program
ASIMP	Aircraft Structural Integrity Management Plan
AU	Acoustic-Ultrasonic
BOS	Baseline Operational Spectrum
BUS	Basic Usage Spectrum
CFH	Component Flight Hours
CS	Certification Sets
CZ/CZM	Cohesive Zone/Cohesive Zone Model
DADT	Durability and Damage Tolerance
DADTA	Durability and Damage Tolerance Assessment
DCB	Double Cantilever Beam
DCPD	Direct Current Potential Drop
DDTCP	Durability and Damage Tolerance Control Plan
DIC	Digital Image Correlation
DVI	Directed Visual Inspection
DSG	Design Service Goal
DSTO	Defence Science & Technology Organization
DT	Damage Tolerance
DTA	Damage Tolerance Analysis
EBH	Equivalent Baseline Hours
EC	Eddy Current
EDM	Electrically Discharged Machining
EIFS	Equivalent Initial Flaw Size
ELE	Estimated Life Expectancy
FCS	Flight Control Surfaces
FE/FEM	Finite Element/Finite Element Analysis
GBS	Grain Boundary Sliding
H-Stab	Horizontal Stabilator
HOLSIP	Holistic Structural Integrity Process
HOWSAT	Hornet Outer Wing Static Testing
HUMS	Health and Usage Monitoring System
ICFT	Integrated Creep-Fatigue Theory

ICSD	Initial Crack Size Distribution
ID	Intragranular Deformation
IFOSTP	International Follow-on Structural Test Program
IR	Infrared
ISRV	Initial Support Readiness Validation
ISS	In-Service Support
KIS	Krack Indicator Sensor
LCF	Low Cycle Fatigue
LEFM	Linear Elastic Fracture Mechanics
LPI	Liquid Penetrant Inspection
MHP	Maritime Helicopter Program
MAPOD	Model-assisted Probability of Detection
MRO	Maintenance, Repair and Overhaul
MSD/MED	Multi-site Fatigue Damage/Multiple Element Damage
NDI/NDE	Non-destructive Inspection/Non-destructive Evaluation
NDT	Non-destructive Testing
OEM	Original Equipment Manufacturer
OLM	Operational Loads Monitoring
POD	Probability of Detection
PSE	Primary Structural Element
RST	Residual Strength Test
SBI	Safety-by-Inspection
SENT	Single Edged Notch Tension
SESC	System Engineering Support Contract
SIF	Stress Intensity Factor
SHM	Structural Health Monitoring
SMP	Structural Maintenance Plan
SRM	Structural Repair Manual
SSI	Structurally Significant Items
TMF	Thermal Mechanical Fatigue
TRL	Technology Readiness Level
TSA	Thermoelastic Stress Analysis
TTCP	The Technical Cooperation Program
UCART	Usage Comparison and Reporting Tool
VCCT	Virtual Crack Closure Technique
WFD	Widespread Fatigue Damage
WRBM	Wing Root Bending Moment

1.0 INTRODUCTION

Canadian Industry, universities and government agencies were solicited for information describing their fatigue technology and structural integrity related activities over the period 2013 to 2015. This review covers work performed or being performed by the following organizations:

Bell Helicopter Textron Canada (BHTC)

Bombardier Aerospace

Department of Mechanical and Aerospace Engineering, Carleton University

Department of Mechanical and Industrial Engineering, Concordia University

Department of National Defence (DND)

- Defence Research and Development Canada (DRDC)
- Royal Canadian Air Force (RCAF)
- Director of Technical Airworthiness and Engineering Support (DTAES)
- Royal Military College of Canada (RMC)

L-3 Communications (Canada) Military Aircraft Services (MAS)

National Research Council Canada (NRC Aerospace)

Names of contributors (where available) and their organizations are included in the text of this review.

Full addresses of the contributors are available through the Canadian National ICAF Delegate at:

Nick Bellinger

Program Leader – Aeronautical Product Development Technologies

National Research Council Canada

1200 Montreal Road, Building M14

Ottawa, ON, K1A 0R6, Canada

Tel: 1-613-993-2410

Email: nick.bellinger@nrc-cnrc.gc.ca

2.0 FULL-SCALE AND COMPONENT TESTING

2.1 CF-18 FLIGHT CONTROL SURFACES LIFE EXTENSION

L-3 Communications (Canada) Military Aircraft Services (MAS)

Historically, the Flight Control Surfaces (FCS) of the CF-18, Figure 2.1, had not been considered systematically as part of the Aircraft Structural Integrity Program (ASIP) effort. The certification basis was demonstrated by the OEM for 6000 Component Flight Hours (CFH). The usage of these components and associated fatigue life had not yet been assessed for a Canadian usage and environment. However, significant work was performed and showed that the fleet was approaching and even exceeding the Original Equipment Manufacturer (OEM) service life limit of 6000 CFH. The Royal Canadian Air Force (RCAF) has taken an interim position to adopt OEM-recommended inspections at 6000 CFH which could potentially be extended to 7000 CFH. Unfortunately this effort is not adequate to meet RCAF fleet requirements.



Figure 2.1 Image of CF-18

Supportability for the fleet until Estimated Life Expectancy (ELE) is a concern, and potential development of sparing and procurement strategies becomes a requirement. Fleet logistic and supportability scenarios show that, to meet fleet ELE, most FCS need to be certified up to 8000 CFH. This would mark the first life extension beyond the OEM service life limit of 7000 CFH attempted by any F/A-18 user and is considered a major certification challenge, particularly in light of aggravating environmental factors that limit the economic life of FCS such as in-service and maintenance induced damages, delaminations, disbonds between the composite skin/core, water ingress, corrosion, etc.

Since ICAF 2013, the global certification strategy for a life extension beyond OEM 6000 CFH has been revised. The certification strategy is primarily based on full scale component testing of the Horizontal STABilator (H-Stab), aileron, inboard leading edge flap and trailing edge flap. L-3 MAS and NRC, the test agency, are currently setting up the various tests. More details for the Horizontal STABilator test is provided in Section 2.3.

The aim is to fatigue test each FCS for 40,000 hours under a fleet representative spectrum. The residual strength test loads will be applied at the end of testing. Each test article will have pre-existing in-service damage such as material degradation due to prolonged environmental exposure (core corrosion, node bond failure, disbonds, etc), aged SRM and nonstandard repairs, delaminations and production defects. The FCS will be installed on a real wing where a number of wing bending load cases will be applied in parallel to the fatigue cycling of FCS's.

It is expected that these tests will provide the necessary data to make a decision on life extension feasibility and clearly identify what fleet maintenance activities are necessary to reach the 8000 hour threshold. This testing effort is planned to be completed by the end of Fiscal Year 2017.

2.2 OUTER WING CERTIFICATION

L-3 Communications (Canada) Military Aircraft Services (MAS)

The outer wing certification has not been demonstrated based on RCAF usage and policy requirements. Prior attempts to bridge certification gaps under component test FT193 were not completely successful and further effort is required. Thus, the remaining outer wing items not certified by previous tests will be addressed through HOWSAT (Hornet Outer Wing Static Testing) residual test program carried out by the Defence Science & Technology Organization (DSTO).

2.3 F/A-18 FT905 CF-18 HORIZONTAL STABILATOR FATIGUE TEST

R.S. Rutledge, NRC Aerospace

Fleet logistic simulations indicate it will be necessary that half the horizontal stabilators in service significantly reach above the original certification limit. In addition, the RCAF fleet inspections have shown that allowable damage sizes have already been exceeded, indicating that the original analytical basis for these components was unnecessarily conservative, particularly considering the complexity of modelling failure in the horizontal stabilator.

Initially, a study was undertaken by NRC, RCAF and L-3 MAS to determine the effect of larger damage sizes on the horizontal stabilator residual strength. A CF-18 2.3 pounds per cubic foot core horizontal stabilator component was statically tested at NRC with induced damages of three increasing sizes at three critical locations to demonstrate the capability of the component to withstand larger damages. An extensive exercise in damage introduction and inspection technique evaluation was carried out. Figure 2.2 illustrates digital image correlation strain measurements used to determine the upper surface strains of the horizontal stabilator on test article ST-312. To establish further confidence following damage introduction and static testing, five once-in-one-lifetime (limit) loads used for the RST testing were applied 2,000 times at each damage location. Using the pulse flash thermography inspection technique, no damage growth was found at any of the three locations during any of the static or cyclic tests.

To ensure fleet operation beyond 2020, to extend the certification basis to meet the new Estimated Life Expectancy of the CF-18 fleet and to avoid expensive horizontal stabilator procurement, the RCAF, NRC and L-3 MAS are performing a structural life extension fatigue test. NRC is in the process of conducting durability and damage tolerance (DADT), and residual

strength testing of a United States Navy retired stabilator with representative service repairs and environmental / fatigue exposure. The stabilator, a hybrid composite skin / aluminium honeycomb core structure, will be durability fatigue tested to the equivalent of five lifetimes of Canadian Forces service usage. The NRC developed loading test rig for conducting this work on test article FT-905 is shown in Figure 2.3. During this portion of testing the stabilator will be inspected at regular intervals to locate and monitor growth of any damages that arise. Upon completion of durability testing, a full characterization of all damages will be undertaken. If required, additional artificial damages of sizes beyond the limits in the current CF-18 Structural Repair Manual will be induced in fatigue prone areas. For the damage tolerance portion, fatigue testing will be conducted to five lifetimes of required life extension while monitoring the above mentioned damages for growth. Residual strength tests to design and ultimate loads are planned at the completion of the DADT testing.

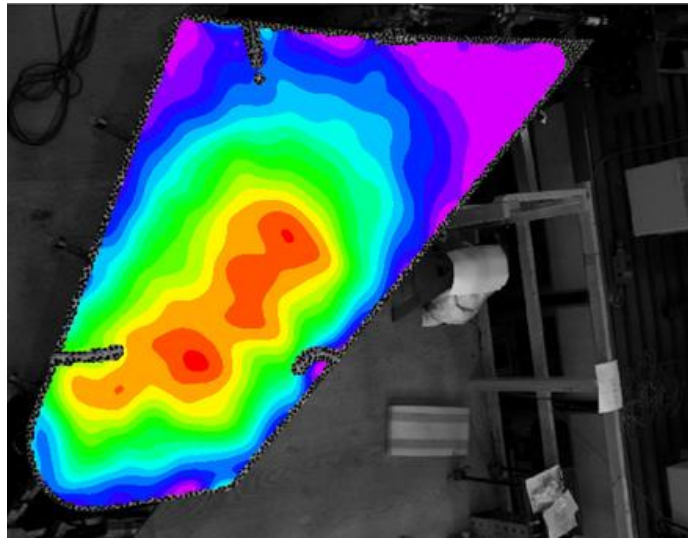


Figure 2.2 Static Test ST-312 Digital Image Correlation Strains

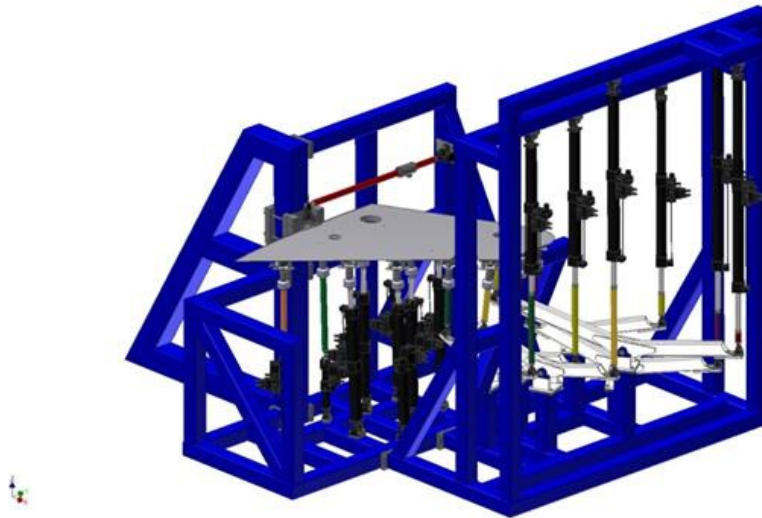


Figure 2.3 Fatigue Testing FT-905 Test Configuration

2.4 DASH-8 MODEL 100 ESP SUMMARY

Bombardier Aerospace

In 2009, a program was undertaken to extend the Dash-8 Model 100 service life from the original certification value of 80,000 Flights to 120,000 Flights. The Dash-8 Model 100 was certified as Damage Tolerant per FAR 25, Amendment 45. As such, the structural maintenance program consists of fatigue damage inspections for the majority of the primary structure with safe-life items limited to the landing gear and its associated support structure on the nacelle, wing and fuselage.

The Dash-8 Model 100 represents the first aircraft for de Havilland (now Bombardier) that was certified damage tolerant. While fatigue testing was done on all major components (full-scale, nacelle, flaps, empennage), as expected, fatigue tests were also done on smaller components to validate durability of the design, develop analytical methods and, for some SSI's, determine the inspection intervals. Not including the major component tests, data from 134 tests would be available to support the extension to 120,000 Flights.

The first phase of the evaluation consisted of defining a minimum aircraft configuration, which identified structural modifications that improve the Airworthiness Limitations but are incorporated at the operator's discretion.

The second phase of the evaluation consisted of sorting the SSI's and Safe-Life items into the following four categories:

1. Structural components, both SSI's and Safe-life items, deemed to be candidates for replacement at 80,000 Flights.
2. SSI's that would require significant re-analysis (typically items cleared by detail test).
3. SSI's that would require minimal re-analysis (typically items cleared through crack growth analysis that may or may not be supplemented by full component or detail test results).
4. SSI's that would require no re-analysis (typically items with low analytical stress levels and/or very long full component or detail test lives).

Category (1) was critical as significant component replacement, especially safe-life items, could have made the program cost prohibitive. Of the 29 SSI's and 19 Safe-Life items initially considered as candidates for replacement, the aforementioned test data, supplemented by crack growth analysis, reduced the mandatory replacement list to four components.

All SSI's were subject to the evaluation for susceptibility to widespread fatigue damage as defined in AC 120-104. Two areas, the lower wing skin between the nacelle and Flap Track #4 and the door stop beams on the Type II and Type III exits, were deemed susceptible. The inspection techniques for the SSI's associated with these areas/components were revised to NDI, instead of DVI, as a result.

Some SSI's have seen a reduction in the Repeat Inspection Intervals as the pre-aging requirement grows a 0.005" MIF for 120,000 Flights of intact structure loading, rather than the original 80,000 Flights.

Parts of a retired high-time Model 100, consisting of a portion of the aft fuse/empennage, a portion of the rear fuselage containing the aft baggage door cut-out, two windows and parts of the circumferential and longitudinal joints and a wing box extending from Yw 0.0 to Yw 250, were obtained for teardown purposes.

Approval by Transport Canada of the Extended Service Program was received in March, 2012 and subsequently EASA. Widerøe's Flyveselskap, Figure 2.4, became the first operator to adopt the Service Bulletins on their fleet of aircraft.



Figure 2.4 Widerøe's Flyveselskap Dash-8-100

Ensuing to those developments, on 2 Feb 2015, Bombardier has committed to do the same type of work on the Dash-8 Series 300 targeted for lead customer Chorus Aviation, Figure 2.5, which operates as Air Canada regional partner Jazz Aviation.



Figure 2.5 Chorus Aviation/ Air Canada Jazz Dash-8-300

2.5 CSERIES DURABILITY AND DAMAGE TOLERANCE TESTS

Bombardier Aerospace

The CSeries complete Aircraft Durability and Damage Tolerance (DADT) test started in mid-August 2014 at IABG in Dresden, Germany, Figure 2.6.



Figure 2.6 CSeries full-scale test in Dresden, Germany

The main objective of the test is to demonstrate the damage tolerance and fatigue characteristics of the metallic components of the CSeries airframe. Other objectives include validation of:

1. Crack growth models for primary metal structure
2. Inspection techniques and intervals
3. Typical repairs and allowable damage limits.

The main components, Figure 2.7, covered by the complete aircraft DADT Test are:

- Complete fuselage including all doors and interfaces
- Centre and outer wing box primary metallic structure
- Vstab & rudder primary metallic structure and interfaces

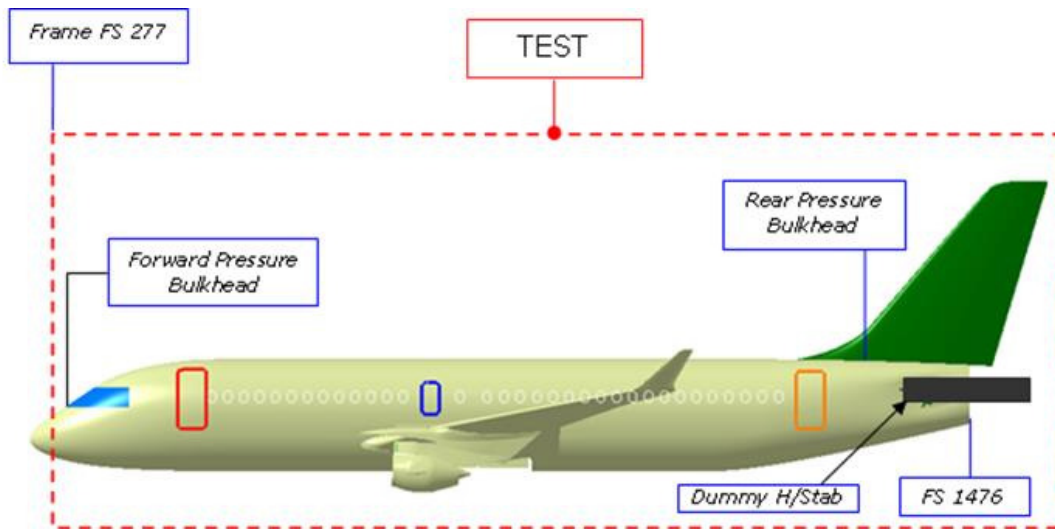


Figure 2.7 Schematic of main CSeries components

The aircraft structure will be subjected to a total of 180,000 flight cycles, which represent three times the Design Service Goal (DSG) of the aircraft. The test program is divided into 3 phases of testing and a final phase for teardown inspection:

1. Phase 1 – Durability testing: Two DSG of flight cycles (120,000 total flights) will be applied to the test article without any artificial damage.
2. Phase 2 – Damage Tolerance Testing: One DSG of flight cycles (60,000 flights for a total accumulated count of 180,000 flights) will be applied to the test article with the presence of artificial damage.
3. Phase 3 – Residual Strength Testing: A series of residual strength tests will be applied to the test article to demonstrate the structural integrity of standard repairs, confirm the critical crack lengths of the Damage Tolerance Analysis and demonstrate freedom from Widespread Fatigue Damage.
4. Phase 4 – Teardown inspection.



Figure 2.8 Close-up of wing test setup



Figure 2.9 Close of fuselage test setup

A mission with four flight types is applied to the test article. This mission was reduced and truncated to an equivalent of 268 end points, on average, per flight. Number of cycles required for Entry-Into-Service was reached at end of Nov 2014. It is expected to reach the end of the first life by end of 2015.

In addition, there are multiples Durability and Damage Tolerance (DADT) Bench Tests for components not covered on the Complete Aircraft DADT Test. Below is a list of the main rigs, Table 2.1. These bench tests will also be tested for 180,000 flight cycles and will follow the same testing program as the Complete Aircraft DADT Test.

Table 2.1 List of subsequent metallic test rigs

TEST RIG (Metallic)
HORIZONTAL STABILIZER AND ELEVATOR DADT TEST
ENGINE PYLON DADT TEST
ENGINE MOUNTS (FWD AND AFT) AND THRUST LINKS DADT TEST
SLAT 2 BODY DADT TEST
SLAT 2 TRACKS DADT TEST
SLAT 4 BODY DADT TEST
WINGLET AND WINGLET ATTACHMENT DADT TEST
INBOARD FLAP BODY DADT TEST
INBOARD FLAP, INBOARD TRACK DADT TEST
OUTBOARD FLAP BODY DADT TEST
OUTBOARD FLAP, INBOARD TRACK DADT TEST
OUTBOARD FLAP, OUTBOARD TRACK DADT TEST
AILERON BODY AND SUPPORTS DADT TEST
GROUND SPOILER DADT TEST
MULTI-FUNCTION SPOILER 1 DADT TEST

As the C Series structure is fabricated utilizing various metal alloys as well as Carbon Fibre Reinforced Plastic (CFRP) for its primary structure, other test rigs are being used to evaluate the durability and damage tolerance characteristics of the composite structure. These rigs are following a different testing program. A list of the main rigs is given in Table 2.2.

Table 2.2 List of composite test rigs

TEST RIG (Composite)
WINGLET AND WINGLET ATTACHMENT DADT TEST
INBOARD FLAP BODY DADT TEST
OUTBOARD FLAP BODY DADT TEST
AILERON BODY AND SUPPORTS DADT TEST
GROUND SPOILER DADT TEST
MULTI-FUNCTION SPOILER 1 DADT TEST
HORIZONTAL STABILIZER AND ELEVATOR DADT TEST
VERTICAL TAIL DADT TEST
WING BOX AND CENTRE WING BOX DADT TEST
BA500 REAR PRESSURE BULKHEAD DADT TEST
AFT FUSELAGE UPPER STRUCTURE DADT TEST

In conclusion, multiple CSeries DADT test rigs started in 2014. Three aircraft design lives (180,000 flight cycles) will be simulated to ensure the metallic structure meet the Damage Tolerance certification requirements, the requirements for Entry-Into-Service as well as the customer expectations.

3.0 PROBABLISTIC AND RISK ANALYSIS METHODS

3.1 INTEGRATED STRUCTURAL LIFE ASSESSMENT TECHNOLOGIES FOR ROYAL CANADIAN AIR FORCE FLEETS*

M. Liao, G. Renaud and Y. Bombardier, NRC Aerospace

*Paper being presented at ICAF2015

A 3-year DRDC-NRC collaborative project (*Integrated Structural Life Assessment for CF Air Fleets*) has been completed and achieved the primary goal of improving and integrating NRC airframe life assessment methodologies and tools (CanGROW, ProDTA, and other supporting tools), including holistic modeling of fatigue, damage tolerance, and age degradation process on new materials (e.g. 7249-T75611) and complex damage modes (MSD/MED/WFD). The detailed results, including developed methods, tests data, and software tools, are documented in over 30 publications, which are listed in Section 3.1.1. The main tasks are highlighted as follows:

Task I: Conduct a brief review/summary of the current CF lifing and risk analysis methods/tools [7][11][34] – conducted a brief review/summary of the existing lifing methods/tools, including risk analysis tools, used by various CF aircraft, and a brief comparison of the CF aircraft lifing methods with other military methods and tools. It is shown that the NRC developed methods/tools have provided significant support to the quantitative risk analyses for various RCAF aircraft fleets (Figure 3.1).

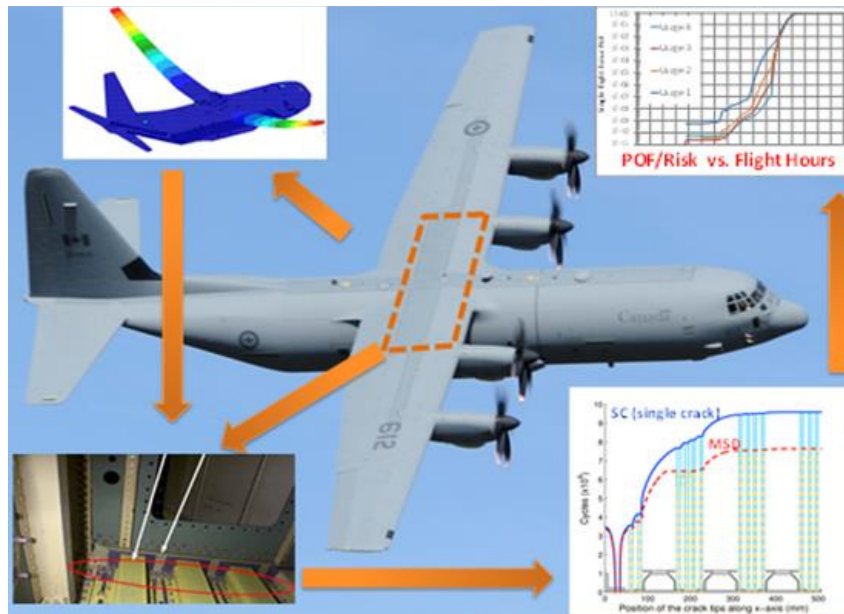


Figure 3.1 Advance risk analysis (CC-130 example) using NRC developed tools (CanGROW and ProDTA)

Task II: Generate fatigue crack growth test data for a new airframe material (7249-T76511) [1][10][14][15][26] [27][28][29][30] – conducted fatigue crack growth rate (FCGR) tests for 7249-T76511 aluminum extrusion (new materials for CP-140), including short-long crack growth tests, low and high stress ratios, under ambient and corrosive environments (Figure 3.2). Basic material characterization tests were carried out on extruded 7249-T76511 aluminum, which includes a limited initial discontinuity state (IDS/particles/pores) study. Fractographic

Review of Canadian Aeronautical Fatigue and Structural Integrity Work 2013-2015

analysis was performed to quantify the crack nucleation features and short crack growth data. These results were used to develop and validate the FCGR material model to support the CF aircraft life assessment. The test data were also shared and used by the OEM (Lockheed Martin) and the RCAF MRO (IMP Aerospace).

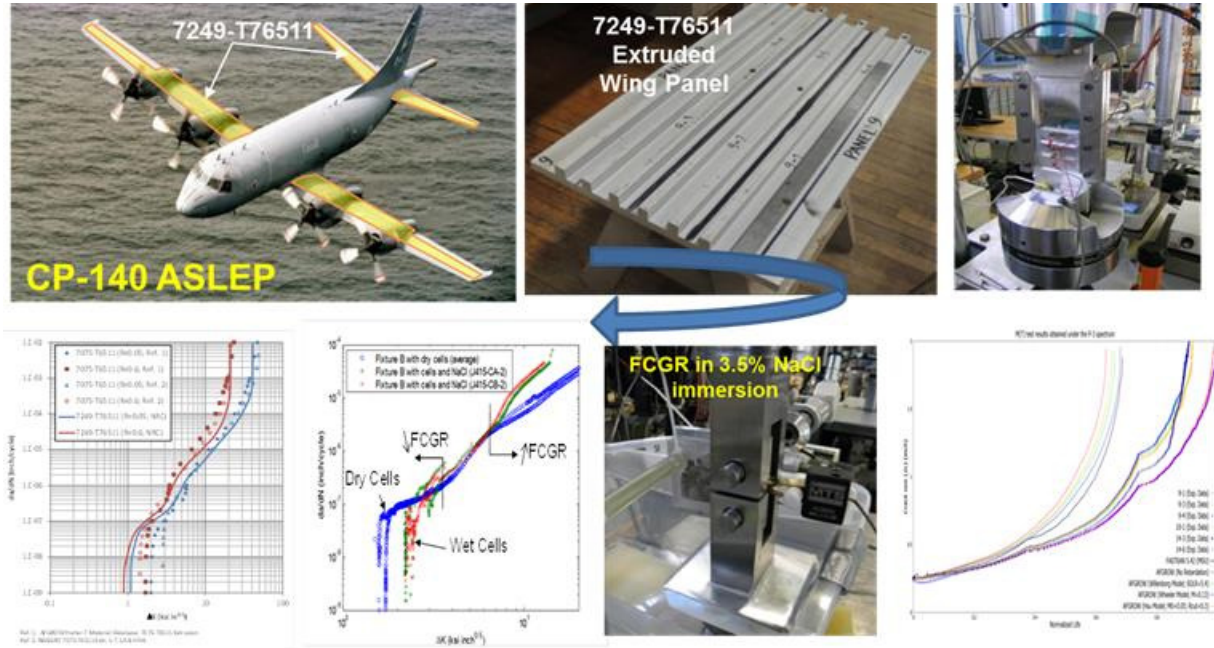


Figure 3.2 7249-T76511 FCGR testing and material model

Task III: Enhance NRC damage tolerance analysis methodologies and tools with expanded beta library and validated material models [1][3][5] [6][18][21] – expanded NRC generic beta-factor library with 3D surface crack solutions. New beta-factors for 1~2 typical fuselage locations considering bulging factor were developed. A graphic user-interface and a post-processor for NRC’s crack growth analysis software, CanGROW was created. New material and retardation models were calibrated with the current test results, and/or existing tests subject to spectrum loading.

Task IV: Improve Global-Local FE methods for multi-load-path structural system with complex damage mode (like MSD/WFD) [8][16][17][33] – improved NRC global-local FEA methods for multi-load-path structural system, with complex damage like MSD/MED for two example locations (wing and fuselage, with focus on fuselage). The NRC simplified FE based generic beta tool with global modelling was validated. The global-local techniques for determining complex stress intensity factors (SIFs) and residual strength including adjacent structural elements (e.g., stringers/caps) failures were improved.

Task V: Improve NRC risk analysis models and tools (ProDTA and CanGROW) for generic fuselage and wing critical locations [7][12][31][32] – developed more efficient computational methods for Monte Carlo crack growth simulation. Optimal ICSD (initial crack size distribution)/EIFS (equivalent initial flaw size) regression method/algorithm along with material as-manufactured initial discontinuity states were developed. The Monte Carlo simulation was improved for inspection with POD and/or POI (probability of inspection) effects,

and/or with repair effects. A preliminary study was conducted on risk-based maintenance optimization with inspection interval, NDI and repair technique options.

Task VI: Demonstrate/validate the developed methods/tools with CF aircraft case studies and best practices [9][13][27][30]– defined the case studies through extensive communication/networking with DTAES and DND contractors. The developed lifing/risk analysis tools were demonstrated on at least one typical fuselage location. The risk analysis tool was improved and updated for the RCAF aircraft structures with a limited number of in-service damage findings. The generic procedures and best practices on structural life and risk analysis for all CF aircraft in support of the RCAF RARM process were reviewed and summarized. The emerging technologies/needs that can be considered for future use in CF lifing concept and development including the HOLSIP framework and prognosis tools using loads or damage data from new monitoring technologies (e.g. SHM) system were explored.

Overall this project provided low TRL testing and modelling results to several Tasks sponsored by DATES for CC-130 and CP-140 fleets, which included higher TRL engineering support and technology transferred to DND and its MROs. As a result, the RCAF air fleets received reliable and timely S&T support on structural life and risk assessment to help decision-making in airworthiness management and cost-effective maintenance, as well as being a smart buyer for the procurement programs on the next generation fighter program and CC-130J centre wing durability testing.

This project has involved some domestic partners like IMP Aerospace, Marshall Aerospace Canada, Royal Military College, University of Waterloo, as well as international partners like Mississippi State University, DSTO, USAF, SwRI and the NASA NASGRO team, and major ASIWG members including Lockheed Martin Aerospace and US Navy. Through the in-kind collaborations, the project outcomes have been recognized by these partners. Collectively this project significantly contributed to three TTCP CPs (under TP4), resulting in the 2014 TTCP Award on “Assessment of Structural life methodologies: C-130 test case”.

3.1.1 REFERENCES

- [1] J. C. Newman, K. F. Walker and M. Liao, Fatigue crack growth in 7249-T76511 aluminium alloy under constant-amplitude and spectrum loading, Article first published online: 13 OCT 2014, DOI: 10.1111/ffe.12253
- [2] Bombardier, Y., Liao, M. and Renaud, G., "Improved Stress Intensity Factor Solution for Cracks in Panels with Arbitrarily Located Stringers", Journal of Aircraft, 2013, Vol.50: 1787-1805, 10.2514/1.C032159.
- [3] Liao, M., Bombardier, Y., Renaud, G., and Bellinger, N.C., Advanced damage tolerance and risk analysis methodologies and tools for aircraft structures containing multiple-site and multiple-element fatigue damages, Proceedings of the Institution of Mechanical Engineers, Part G: Journal of Aerospace Engineering, November 2012 226: pp. 1412-1423.
- [4] Bombardier, Y., and Liao, M., A New Stress Intensity Factor Solution for Cracks at an Offset Loaded Fastener Hole, Vol.48, No.3 Journal of Aircraft, May-June 2011, pp. 910-918.

- [5] Bombardier, Y., Liao, M., Displacement Field in a Stringer Subjected to a Pair of Fastener Loads, Publication Number: LTR-SMPL-2011-0159
- [6] Renaud, G., Liao, M., Bulging Factor Solutions for Cracks in Pressurized Fuselage Panels: A Preliminary Study, Publication Number: LTR-SMPL-2011-0246
- [7] Liao, M., A Critical Review of the Single Flight (Hour) Probability of Failure (SFPOF) for Aircraft Structural Risk Analysis, Publication Number: LTR-SMPL-2012-0022
- [8] Li, G., Renaud, G., and Liao, M., Analysis of load profile at the CC-130 CW-1 critical location using global finite element modelling, LTR-SMPL-2012-0100
- [9] Renaud, G., Liao, M., Calibration of AFGROW and CanGROW Models Using the CP-140 SLAP Test Results, Publication Number: LTR-SMPL-2012-0154
- [10] Bombardier, Y., Liao, M., Backman, D., Fatigue Crack Growth Rate Testing of 7249-T76511 Aluminium, Publication Number: LTR-SMPL-2013-0001
- [11] Liao, M., Renaud, G., Bombardier, Y., Review of Fatigue Life Assessment Methods for Aircraft Structures, Publication Number: LTR-SMPL-2013-0057
- [12] Renaud, G., Bombardier, Y., Liao, M., Development of Equivalent Initial Flaw Sizes for Single and Multiple Site Damage, Publication Number: LTR-SMPL-2013-0066
- [13] Liao, M., Renaud, G., Bombardier, Y., Evaluation of Fatigue Crack Growth Analysis Tools using C-130J Coupon Tests, Publication Number: LTR-SMPL-2013-0144
- [14] Bombardier, Y. and Liao, M. "Fatigue Crack Growth Rate Testing of 7249-T76511 Aluminum Alloy for Naturally Nucleating Cracks", LTR-SMM-2014-0001, 7/7/2014.
- [15] Bombardier, Y., Liao, M., Fatigue Life Improvement Factor of Cold Worked Holes for the CP-140/P-3 Outer Wing Assembly, LTR-SMM-2014-0019
- [16] Li, G., Renaud G. and Liao, M. Strain life prediction for a flat panel using global/local FEM LTR-SMM-2014-0096, 6/19/2014
- [17] Renaud, G. Li, G. and Liao, M. Strain life analysis of a curved panel using global/local FEM, LTR-SMM-2014-0091, 7/7/2014
- [18] Bombardier, Y., Liao, M., Renaud, G., CanGROW for Windows - User Guide (Version 1.1), Publication Number: LTR-SMPL-2013-0148
- [19] Liao, M., Comparison of Different Single Flight Probability of Failure Calculations for Aircraft Structural Risk Analysis, to be presented at 2012 Aircraft Airworthiness & Sustainment Conference (AA&S2012), Baltimore USA, April 2012.
- [20] Bombardier, Y., Liao, M., Renaud, G., Improved stress intensity factor solution for cracks in panels with arbitrarily located stringers, 53rd AIAA/ASME/ASCE/AHS/ASC Structures, Structural Dynamics and Materials Conference, 4/23/2012 To 4/26/2012, Honolulu, Hawaii.
- [21] Renaud, G., Liao, M.; Improved Stress Intensity Factor Solutions for Surface and Corner Cracks at a Hole, 53rd AIAA/ASME/ASCE/AHS/ASC Structures, Structural Dynamics and Materials Conference, From 4/23/2012 To 4/26/2012, Honolulu, Hawaii.
- [22] Liao, M., Renaud, G., Bombardier, Y., Desnoyers, R., Benak, T., Short/Small Crack Model Development for Aircraft Structural Life Assessment, The 13th International Conference on Fracture ICF13, Beijing, China, June 2013.

- [23] Liao, M., Renaud, G., Bombardier, Y., Bellinger, N., Probabilistic Risk Analysis for Aircraft Structural Life Assessment with Limited In-Service Damage Findings, The 28th Congress of the International Council of the Aeronautical Sciences (ICAS 2012), 23-28 September 2012, Brisbane, Australia.
- [24] Bombardier, Y. and Liao, M., Renaud, G., Fatigue Crack Growth Testing and Modelling of 7249-T76511 Aluminium Alloy, The 4th annual Aircraft Airworthiness & Sustainment Conference (AA&S 2013) From 3/25/2013 To 3/28/2013, Grapevine, Texas, USA.
- [25] Renaud, G., Liao, M., Bombardier, Y., Calculations of Equivalent Initial Flaw Size Distributions for Multiple Site Damage, The 4th annual Aircraft Airworthiness & Sustainment Conference (AA&S 2013) From 3/25/2013 To 3/28/2013, Grapevine, Texas, USA.
- [26] Bombardier, Y. and Liao, M., "Fatigue Crack Growth Testing and Modelling of 7249-T76511 Aluminium Alloy", CASI 60th Aeronautics Conference and AGM Aerospace Clusters (AERO 13) April 30, 2013 to May 2, 2013, Toronto, Ontario, Canada.
- [27] Bombardier, Y., Liao, M., Development of a Fatigue Crack Growth Rate Material Model for 7249-T76511 Aluminum Alloy, Thirteenth International ASTM/ESIS Symposium on Fatigue and Fracture Mechanics (39th National Symposium on Fatigue and Fracture Mechanics), November 2013, Jacksonville, USA.
- [28] Newman, J. C., Walker, K., Liao, M., Fatigue Crack Growth Tests and Analyses on 7249-T76511 Aluminum Alloy Specimens under Constant-Amplitude and Simulated Aircraft Wing Loading, ASTM/ESIS Fatigue and Fracture Mechanics Symposium, Jacksonville, FL, November 13-15, 2013
- [29] Liao, M., Bombardier, Y., "Fatigue Crack Growth Testing and Modelling of 7249-T76511 Aluminium Alloy", P-3 ASIWG Conference by USN, RCAF, GN (German Navy), RAAF, RNoAF. Atlanta, USA, 2013.
- [30] Bombardier, Y. and Liao, M., "Fatigue Crack Growth Rate Testing and Modeling of 7249-T76511 Aluminum Alloy", 2014 Aircraft Airworthiness and Sustainment (AA&S) Conference From 4/14/2014 To 4/17/2014., Baltimore, Maryland, USA.
- [31] Renaud, G., Liao, M., Bombardier, Y., Monte Carlo Based Quantitative Risk Assessment for Multiple Site Damage in Aircraft Structures, 2014 Aircraft Airworthiness and Sustainment (AA&S) Conference From 4/14/2014 To 4/17/2014., Baltimore, Maryland, USA.
- [32] Renaud, G., Liao, M. and Bombardier, Y., "Calculation of Equivalent Initial Flaw Size Distributions for Multiple-Site Damage", SciTech 2014 (including the 55th AIAA/ASME/ASCE/AHS/ASC Structures, Structural Dynamics, and Materials Conference) From 1/13/2014 To 1/17/2014., National Harbor, Maryland, USA, CPR-SMPL-2013-0147, 11/25/2013
- [33] Renaud, G., Li, G., Shi, G., Bombardier, Y., and Liao, Y., "Analysis of a Lap Joint Including Fastener Hole Residual Stress Effects, AFGROW Workshop 2014, Layton, UT, September 9-10 2014.

[34] Liao, M., Kainth, T., Renaud, G., Bombardier, Y Quantitative Risk Analysis to Support Continued Airworthiness Management, Publication Number, NATO-RTO-AVT-222, Brussels, Belgium, October 2014.

3.2 DEVELOPMENT OF IMPROVED METHODOLOGIES FOR MULTIPLE SITE DAMAGE TOLERANCE ANALYSIS

G. Renaud, M. Liao and Y. Bombardier, NRC Aerospace

A methodology was developed to calculate equivalent initial flaw sizes (EIFS) consistent with multiple-site damage in-service findings [1]. It involves a numerical optimization process in which an EIFS is calculated for each individual crack site, taking into account the simultaneous growth at all crack nucleation sites. It was compared with a simplified single-crack engineering approach that was previously used by NRC for structural risk analysis. Calculated EIFS, fatigue life, and risk results resulting from both approaches were compared for the RCAF in-service damage and nil findings at the CC-130 CW-1 location. It was found that the proposed MSD EIFS calculation approach could give shorter or longer lives, depending on the type of problem and the modeling assumptions. Also, the proposed MSD methodology, which does not modify the state of in-service findings, could potentially reduce inspection and maintenance costs.

To complement the MSD EIFS calculations, an analysis method was developed to improve residual strength (RS) calculation for MSD scenarios [2] (Figure 3.3). As opposed to the traditional approach that considers a single residual strength curve by assuming a predetermined lead crack link-up sequence (the “worst” MSD sequence), the new method generates different curves for different Monte Carlo simulations. In this way, the single “RS vs. lead crack length” relationship is replaced by multiple “RS vs. time” relationships, for which the most critical lead crack can vary based on any realistic crack nucleation scenario.

- **MSD Residual Strength Calculation**

- Cracking sequence can be different for each Monte Carlo trial
- Modified approach in ProDTA
- Complement MSD EIFSD calcs.

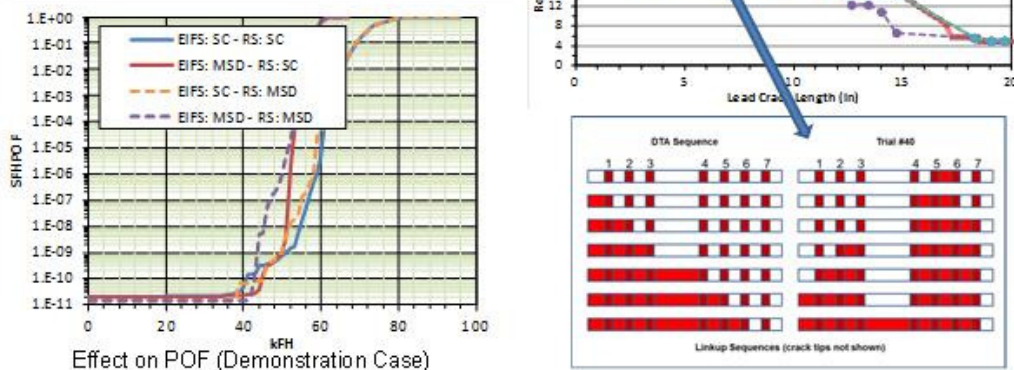


Figure 3.3 Improved MSD residual strength calculation method

3.2.1 REFERENCES

- [1] Renaud, G., Liao, M. and Bombardier, Y., “Calculation of Equivalent Initial Flaw Size Distributions for Multiple-Site Damage”, SciTech 2014 (including the 55th AIAA/ASME/ASCE/AHS/ASC Structures, Structural Dynamics, and Materials Conference), 13-17 January 2014, National Harbor, Maryland, USA.
- [2] Renaud, G., Liao, M., Bombardier, Y., “Monte Carlo Based Quantitative Risk Assessment for Multiple Site Damage in Aircraft Structures”, 2014 Aircraft Airworthiness and Sustainment (AA&S) Conference From, 14-17 April 2014, Baltimore, Maryland, USA.

3.3 DEVELOPMENT OF AN IN-SERVICE DAMAGE ASSESSMENT TOOL

G. Renaud and M. Liao, NRC Aerospace

A tool (Figure 3.4) was developed to allow the RCAF to carry out periodic independent statistical analyses of in-service findings (damaged cracks and nil findings). This tool, able to duplicate analyses performed by the OEM, was used to compare two estimations of the historical usage of the CC-130. It showed, by comparing regressed censored EIFS distributions with that from another operator, that a structural modification performed in the 1980’s can be assumed to have restored the initial hole quality [1].

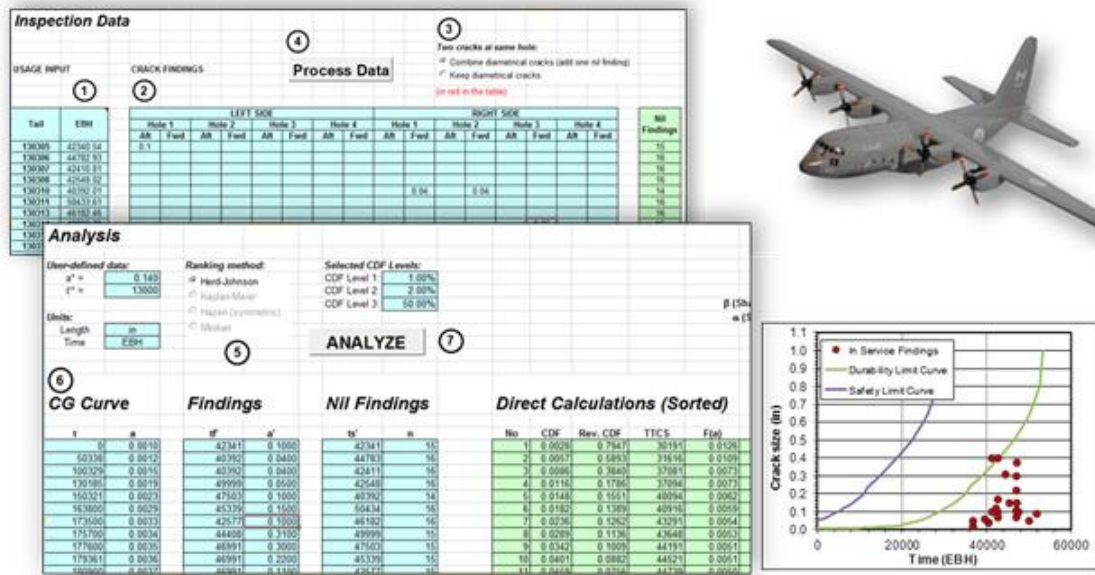


Figure 3.4 NRC In-Service Damage Regression Tool

3.3.1 REFERENCES

- [1] Renaud, G., Liao, M., Bombardier, Y., “Effect of a Structural Modification on the Life Estimation and Probability of Failure of the CC-130 Center Wing”, 2015 Aircraft Airworthiness and Sustainment (AA&S) Conference From, 30 March - 2 April 2014, Baltimore, Maryland, USA.

3.4 FATIGUE LIFE IMPROVEMENT FACTOR OF COLD WORKED HOLES FOR THE CP-140/P-3 OUTER WING ASSEMBLY

Y. Bombardier and M. Liao, NRC Aerospace

The cold working method is generally recognized to improve the fatigue crack growth life of metallic aircraft structures. The level of life improvement depends on several factors, such as the material, the geometry of the structure, the loading spectrum, and the cold working procedure. Despite this, the life improvement factor is often assumed based on generic test results, which may not be representative of the CP-140/P-3 aircraft structures where cold working is used. This had led to the need to perform coupon testing to quantify the life improvement factors for CP-140/P-3 specific locations.

The objective of this test program was to quantify the cold work versus non cold work crack growth life improvement associated with split sleeve cold working as applied to open holes subjected to CP-140/P-3 specific airframe spectra. Fatigue tests were conducted on coupons machined from Al 7249-T76511 extruded wing panels. The coupon geometry included a hole with a radial notch to be more representative of the front beam holes of the CP-140/P-3 outer wing assembly. The test matrix included 12 specimens: 6 baseline specimens and 6 cold worked specimens.

Crack size was monitored using the direct current potential drop (DCPD) technique and visual measurements. Since no DCPD formula was available in literature for a radial crack at a hole, some exploratory research effort was carried out and a new equation has been proposed:

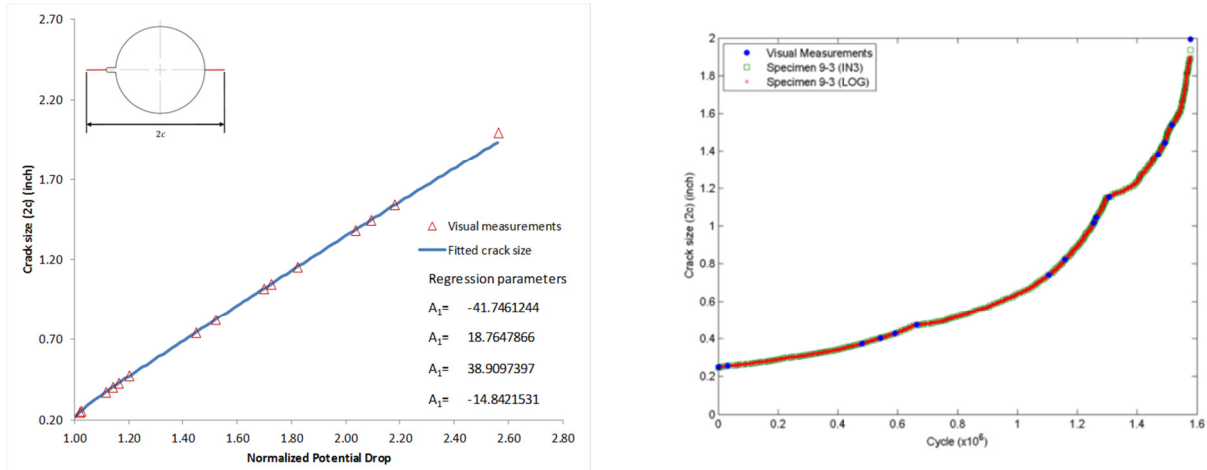
$$\left(\frac{c}{c_0}\right)^2 = A_1 + A_2(PD_n)^2 + A_3(PD_n)^{-2} + A_4(PD_n)^{-4}$$

$$PD_n = \left(\frac{PD_a}{PD_{a0}}\right) \left(\frac{PD_{r0}}{PD_r}\right)$$

where

PD_n	Normalized potential drop (corrected)
PD_a	Potential drop measured from the active probes
PD_{a0}	Initial potential drop measured from the active probes
PD_r	Potential drop measured from the reference probes
PD_{r0}	Initial potential drop measured from the reference probes
c_0	Half initial crack size
c	Half current crack size
A_1, A_2, A_3, A_4	Regression parameters

The DCPD equation fitting process to visual measurements is illustrated in Figure 3.5a, which resulted in the crack size measurements shown in Figure 3.5b. For this example, the relative error between the visual and DCPD crack size measurements was within 0.6%, except for the last visual measurement just before failure.



a) Fitting of DCPD equation to visual measurements

b) Comparison between DCPD crack size measurements to visual measurements

Figure 3.5 Typical DCPD crack size measurements results

The fatigue test results indicates that the life improvement factor associated with split sleeve cold working, as applied to open holes subjected to P-3 specific airframe spectra, is larger than 4.0.

3.4.1 REFERENCE

- [1] Bombardier, Y., Liao, M., Fatigue Life Improvement Factor of Cold Worked Holes for the CP-140/P-3 Outer Wing Assembly, LTR-SMM-2014-0019

4.0 STRUCTURAL INTEGRITY

4.1 CT114 (TUTOR) AIRCRAFT STRUCTURAL INTEGRITY PROGRAM (ASIP)

L-3 Communications (Canada) Military Aircraft Services (MAS)

L-3 MAS conducts a full-fledged ASIP program on the CT114 Tutor fleet, Figure 4.1, on behalf of the RCAF. The CT114 ASIP includes the following major tasks:

- Prepare and keep up-to-date the ASIP Master Plan (known as Aircraft Structural Integrity Management Plan – ASIMP in the Technical Airworthiness Manual),
- Prepare and keep up-to-date supporting plans; such as the Structural Maintenance Plan (SMP), Durability and Damage Tolerance Control Plan (DDTCP), and Structurally Significant Items (SSI) database,
- Monitor fleet usage by collecting, processing aircraft usage information, calculating consumed fatigue life, estimating remaining structural life for each aircraft, and providing periodic reports to DND.



Figure 4.1 CT114 Tutor

Aircraft usage monitoring is achieved by collecting, evaluating and processing the Operational Loads Monitoring (OLM) system data. Periodically, collected aircraft usage data is validated and accumulated fatigue damage is calculated for major aircraft components. In addition, remaining life for every major aircraft component is calculated based on predicted aircraft usage by using the software tool GIFTS. The monitoring program findings and L-3 MAS recommendations are reported to DND on a bi-monthly basis.

Additional efforts are also planned to start evaluating the potential for further extension of the service life of the Tutor fleet. This will involve a review of current SSI inspection requirements, identification of additional SSI requiring inspection/rework and the development of a Fleet Strategy to manage the rotation of service aircraft with those in storage in order to meet the new planned retirement date.

4.2 S-92 MARITIME HELICOPTER (CYCLONE)

L-3 Communications (Canada) Military Aircraft Services (MAS)

As part of the Maritime Helicopter Program, L-3 MAS is mandated to conduct an ASIP program on the S-92, designated as CH-148, Cyclone, by the RCAF, Figure 4.2. As part of the Initial Support Readiness Validation (ISRV), L-3 is currently setting up and validating the capabilities to perform structural condition monitoring and usage monitoring.



Figure 4.2 CH-148 Cyclone Helicopter

Usage monitoring will be enabled via the S-92 Health and Usage Monitoring System (HUMS). The HUMS has the capability to recognize flight regimes and manoeuvres via recorded flight parameters and sensor data. This data is processed by the Usage Comparison and Reporting Tool (UCART) that computes fatigue damage rates at various locations. Damage rates as well as statistics at either the mission type or manoeuvre/regime level are then compiled for each individual aircraft and compared to the design spectrum according to the requirements of MIL-STD-1530.

The other major component of the CH-148 ASIP Program is the Structurally Significant Item (SSI) database. The SSI database records all the relevant information about each SSI, also known as Primary Structural Element (PSE), from the design phase and into the in-service phase in order to enable ASIP analysts to monitor structural defects and, when needed, recommend changes to the maintenance program or modifications to the helicopter.

4.3 CF-18 AIRCRAFT STRUCTURAL INTEGRITY PROGRAM (ASIP) AND LIFE EXTENSION PROGRAM (ALEX)

L-3 Communications (Canada) Military Aircraft Services (MAS)

L-3 MAS conducts a full-fledged ASIP program on the CF-18 fleet on behalf of the RCAF. Most of the recent efforts are dedicated towards interpretation of the IFOSTP full scale testing, Aircraft Sampling Inspections (ASI), and fleet findings (RCAF and other operators) in order to define and update the Structural Maintenance Program (SMP) of the aircraft, more specifically, the ALEX Program. Considering the RCAF Baseline Operational Spectrum (BOS) and increased scatter factors, ALEX represents a 50% extension in life over the original design life definition/specification.

L-3 MAS has finalized the definition and development of the third phase of the ALEX program, designated as CP3. To that end, over 340 fatigue and damage tolerance analyses have been conducted since 2006. In many instances, life-limited areas could not be substantiated using safe-life principles and were assessed against the airworthiness and logistic risk analysis methodologies adopted by the RCAF in order to decide on the mitigation strategy or, in some instances, provide substantiation for acceptance of the risk. CP3 includes 61 maintenance packages to be implemented at around 80% of the service life of the aircraft. The CP3 Validation and Verification aircraft was inducted and delivered in 2012.

While the first two phases of ALEX concentrated largely on preventative modifications aimed at meeting the safe-life criteria, CP3 is primarily a safety-by-inspection program comprised mostly of one-time or recurring inspections and on-condition repairs. This apparent change in philosophy from safe-life to safety-by-inspection results from the application of the RCAF logistic risk process where these two options are assessed, on a case-by-case basis, in terms of their cost and downtime impact, accounting for anticipated failure rates.

Now that the ALEX CP3 program is underway, current efforts are directed towards a detailed review of the completion of the CF-18 Structures Certification status to ensure safe operation until fleet retirement. The aircraft structure is broken down in sub-sections (referred to as Certification Sets or CS), based on main loading acting affecting each area, and these sub-sections are reviewed to determine if the IFOSTP provides the means to demonstrate compliance to RCAF certification requirements at all areas of the aircraft based on current usage and if this is shown to not be the case, to identify where gaps may exist in the particular CS. In this aim, all available sources of data are considered including full scale testing, component testing, localized coupon testing results and various options to be addressed analytically. This work is considered critical as it must account for the planned ELE (Estimated Life Expectancy) of the CF-18 fleet which was formally announced as being extended to 2025 vs. the prior ELE of 2020. This fact alone provides a substantial challenge in terms of certification of the aircraft, particularly for components (CS's) on the airframe where fatigue accrual is not necessarily proportional to conventional "G-loading" but is affected by other parameters as will be discussed in the next paragraph. Regardless however, in the case where certification gaps have been identified relative to the current usage/ELE, various options are investigated to address the gaps including component testing, static and residual strength testing, Safety-by-Inspection (SBI) alternatives as well as various analytical approaches.

Part of the reasons for this certification review is to assess the impact of changes in the usage of the CF-18 fleet over the years. Multiple studies were performed to evaluate how much the severity of key interface loading has evolved compared to the Wing Root Bending Moment (WRBM), which is the main interface load being monitored on every aircraft of the fleet. This review highlighted that some interface loads have increased in usage severity much more than the WRBM, and therefore might not be tracked adequately in-service or be certified by past tests. Examples of interface loads that were not tested so as to represent current usage include the reversed (or negative) N_z and negative-WRBM, aileron and horizontal tail usage which are more severe under the current usage than on certification tests. Other reasons include failure modes

found in-service that were not covered during the certification test programs (e.g. stress corrosion cracking, corrosion, impact damage on composite structure, environmental damage, etc.).

All the main structural components in a CS are being reviewed to assess the certification status in terms of main loading, test coverage, in-service issues, modification/repair status, etc. The gaps identified for every component are being documented and option analyses are considered to select the most appropriate. Small certification gaps (i.e. areas tested using proper loads but slightly under tested, etc.) can probably be addressed through some additional analytical work and/or risk assessment. On the other hand, areas that were seriously under tested (e.g. dynamic loads not well represented during test, or responding to loads that were not represented adequately (e.g. Wing Torque), etc.) will probably require some additional testing or development of Safety-by-inspection approach or modification of the area to comply with the certification requirements. Lastly, areas that have been shown to be predominately influenced by dynamic loads were often under-tested in terms of overall cycling duration during IFOSTP.

Based on these CS reviews, many areas requiring additional certification efforts have been identified and are in the process of being addressed. Some specific test programs are being developed to address localised issues at some key components. An example of such tests is discussed in Section 2 for the flight control surfaces and also outer wing certification.

4.4 F-18 INTERNATIONAL SUPPORT

L-3 Communications (Canada) Military Aircraft Services (MAS)

L-3 MAS is supporting the United States Navy in their life extension efforts for those late-lot F/A-18C and D aircraft that did not receive Centre Barrel Replacements. This is being accomplished through a series of discrete modifications which have been shown to be significantly more cost-effective than replacement of several major components. This will be accomplished via the development of localized preventative modifications which utilize robotic shot-peening to provide the necessary life improvements to meet the desired service life of the aircraft. The use of robotic equipment is mandatory under USN regulations to ensure a repetitive peening quality for which a certified life improvement factor can be demonstrated.

To demonstrate this life improvement, a shot peening coupon test program has been undertaken with the National Research Council (NRC) Canada as the testing agency. A very significant amount of coupons (over 200) are planned to verify the effect of all parameters involved in the shot peening of these various modifications (material, geometry, stress level, amount of pre-cycling, etc.) which will provide a very solid foundation for substantiating late incorporation of shot peening on military A/C parts. Note that prior to shot peening, a light blend is performed on the surface to be peened to at least remove the pre-IVD etching applied at production of the airplane that have generated small fatigue defects over time. The test program will also define how much material needs to be removed to ensure shot peening works well even at up to 80% or more of the unfactored life of a given hot spot.

The use of robotic equipment not only allows a consistent quality but facilitates the physical implementation of these modifications in confined areas, previously inaccessible such as the internal fuel tank of the F/A-18 where production personnel would have difficulties in conducting the required operations. Figures 4.3 and 4.4 for representation of the F-18 fuel tank rework area in which some of these mods will be applied. L-3 MAS is currently contracted to complete the Non-Recurring Effort of these mods as well as to develop, manufacture and deliver all the tooling and robotic system/codes required for the incorporation of these retrofits in the USN fleet.



Figure 4.3 F/A-18 Fuselage Fuel Tank

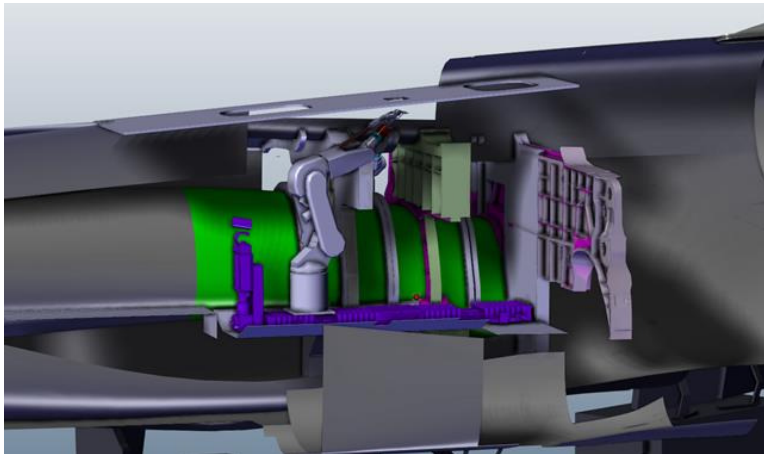


Figure 4.4 Robot Shot Peening Inside F/A-18 Fuel Tank

4.5 MULTI-PURPOSE ATMOSPHERIC PLASMA FOR PAINT STRIPPING AND ENHANCED LPI

C. Li and M. Yanishevsky, NRC Aerospace

Paint stripping and subsequent non-destructive inspection using Liquid Penetrant Inspection (LPI) has been routinely used by the RCAF to assist in aircraft maintenance and repair. Studies have found that conventional methods such as chemical paint stripping and media blasting

present not only environmental and safety issues, but they also mask the indications of surface cracks due to entrapped media or residues from the strippers. Other routine methods such as hand sanding remove partial surface indications of cracks along with the paint, compromising the ability to reliably assess the damage and aircraft structural integrity.

Atmospheric plasma, a multi-purpose next generation technology for aircraft repair and maintenance, has demonstrated good potential for paint/coating removal, surface preparation for non-destructive inspection (NDI), as well as surface preparation for bonding. This non-contact, media-free technology allows for removal of paints and sealants from aircraft structures in an exceptionally controlled manner. Recent results from United States Air Force (USAF) trials showed that atmospheric plasma led to significantly improved detection rates of surface cracks using LPI indications, with 100% detection of cracks as compared to less than 50% from conventional paint stripping methods [1]. Atmospheric plasma technology requires only standard power supply and a dry compressed air source, making it portable and field deployable. Another advantage of this novel technology is its inherent scalability. The United States Navy (USN) is currently looking into its application for paint stripping of large naval platforms [2].

As part of a DND green initiative for aircraft repair and maintenance, NRC has been tasked to investigate the potential of this novel technology. The primary purpose of the proposed work is to evaluate priorities for the application of atmospheric plasma technology by the Department of National Defence (DND), to conduct research to determine and optimize atmospheric plasma process parameters for the studied applications and to determine the impact of the process on the environment and the performance of materials of interest.

To date, NRC has developed a priority list of materials and paint schemes utilized on Canadian Forces aircraft. Several potential suppliers of atmospheric plasma technology for surface preparation and depainting have been evaluated using small coupons. A depainting system has been purchased and it is currently being commissioned to enable undertaking of this study. Large size flat test panels are in the final stages of preparation / painting at the DND Quality Engineering Test Establishment to military aircraft painting specifications. NRC has also developed a test protocol for evaluating the condition of the substrates and primer / paint layers before and after depainting. Following development and validation of the atmospheric plasma depaint process on simple flat panels, panels with artificially seeded fatigue cracks emanating from fastener holes, introduced after painting, will be depainted using this technology, and the impact on Liquid Penetrant Inspection evaluated in comparison with other currently used depaint technologies.

4.5.1 REFERENCES

- [1] N. Tracy, Nondestructive Evaluations (NDE) Exploratory Development for Air Force Systems, AFRL-RX-WP-TR-2010-4200, Dec 2009.
- [2] P. Yancey, Media Free Coating Removal Technology for Navy Platforms using Atmospheric Plasma, Sol NO. Navy SBIR FY2009.1, 2009.

4.6 SAFETY CUTS IN FATIGUE DAMAGED FASTENER HOLES

J. Juurlink, D. DuQuesnay, Royal Military College of Canada/Directorate of Technical Airworthiness and Engineering Support.

An investigation into the effectiveness of safety cuts repair practises during fatigue damage removal from fastener holes in aircraft structures was conducted to better define future repair methodology for the RCAF. Current repair practises include a 0.030 inch safety cut in order to reduce the potential of residual cracks in the repaired structure. However, safety cuts reduce the cross section of the structure and decrease edge margins, subsequently increasing the local stresses around the repair. If safety cuts can be limited or eliminated from fatigue damage repairs, it may allow for an increase in fatigue life of the remaining structure post-repair.

Experimental coupons were machined to best represent legacy aircraft thin metallic components with characteristic fastener holes. Canadian Forces trained technicians performed all inspection and removal procedures on fatigue damage contained within the holes as per current procedural standards. Experimentation focused on two critical issues with respect to aircraft repair: the inspection and probability of detection of existing cracks as well as the methods of repair and their effect on final fatigue life. Specifically, the effects of employing a 0.015 inch radial safety cut in comparison to a benchmark coupon excluding the safety cut.

All specimens were tested in fatigue under constant amplitude loading at a load ratio of zero, Figure 4.5. After reviewing the effects of a safety cut on fatigue life in comparison to the benchmark, results supported the use of a 0.015 inch safety as an effective means of repairing fatigue damage. The current data set indicates that there is no evidence that safety cuts are detrimental to fatigue life of the coupons.

The utilization of two non-destructive inspection techniques provided a probability of detection $a_{90/95}$ of approximately 0.010 inches. Residual cracks, contained within nine of the twenty coupons that were not safety cut, significantly decreased the fatigue life of subsequent fatigue tests. Conversely, the advantage expected from a greater cross section in the non-safety cut coupons was not seen. Despite having a larger cross section and subsequently lower net stresses than specimens with safety cuts, the data showed safety cut coupons have equal or greater fatigue lives than non-safety cut coupons.

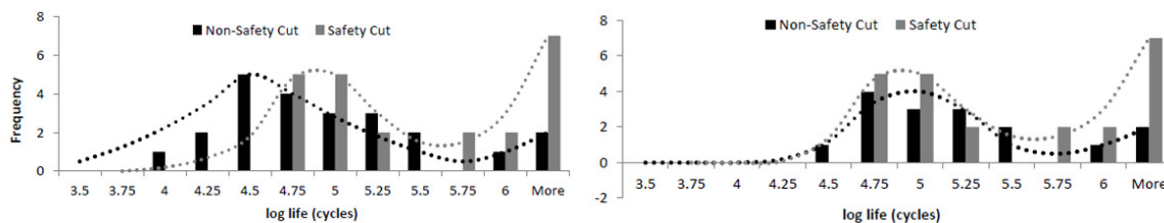


Figure 4.5 Distribution of Post-Repair Fatigue life of Fatigue tested Coupons: Including and Excluding Post-repaired Coupons containing Residual Cracks

In addition to the primary objectives, it was found that the surface finish left by the repair procedure, Figure 4.6, played a greater role in final fatigue life than originally expected. In cases where machining surface defects were co-located with regions of higher stress concentrations, fatigue cracks formed significantly sooner.

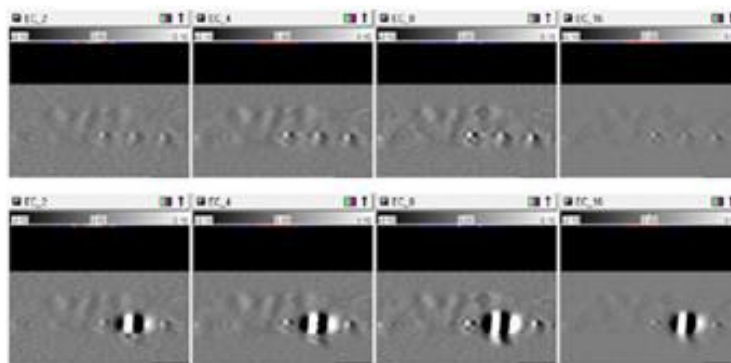


Figure 4.6 Effects of Surface Defects created during Repair Procedures as shown via the MultiView 6.1 Eddy Current Signal display at approximately 0 and 50,000 Cycles

4.7 FATIGUE PERFORMANCE CHARACTERIZATION OF A COMPOSITE BUTT JOINT CONFIGURATION

G. Li, NRC Aerospace

Although there exists an extensive literature base and knowledge on laminated composites, information is still lacking for specific joint configurations. For instance, there is limited knowledge on the static strength and fatigue performance found for single-strap (or single-doubler) joint configurations. To support failure analyses of pre-cured fuselage composite joints for the new generation of aircraft, the associated data needs to be established in order to provide a solid basis for the advanced joint design work. The single-strap joint configuration can act as a baseline to develop other relevant joints for aircraft composite fuselage structures, with an appropriate attachment ensuring joint structural integrity, Figure 4.7. The main objective of the present study was to quantitatively examine the fatigue performance of the composite butt joint configuration under specific conditions and associated joint failure mode, damage evolution, and stiffness degradation. The specific conditions examined include laminate layup sequence (with either 0° or 45° surface ply orientation), doubler thickness (i.e. bending stiffness), joint attachment, and damage.

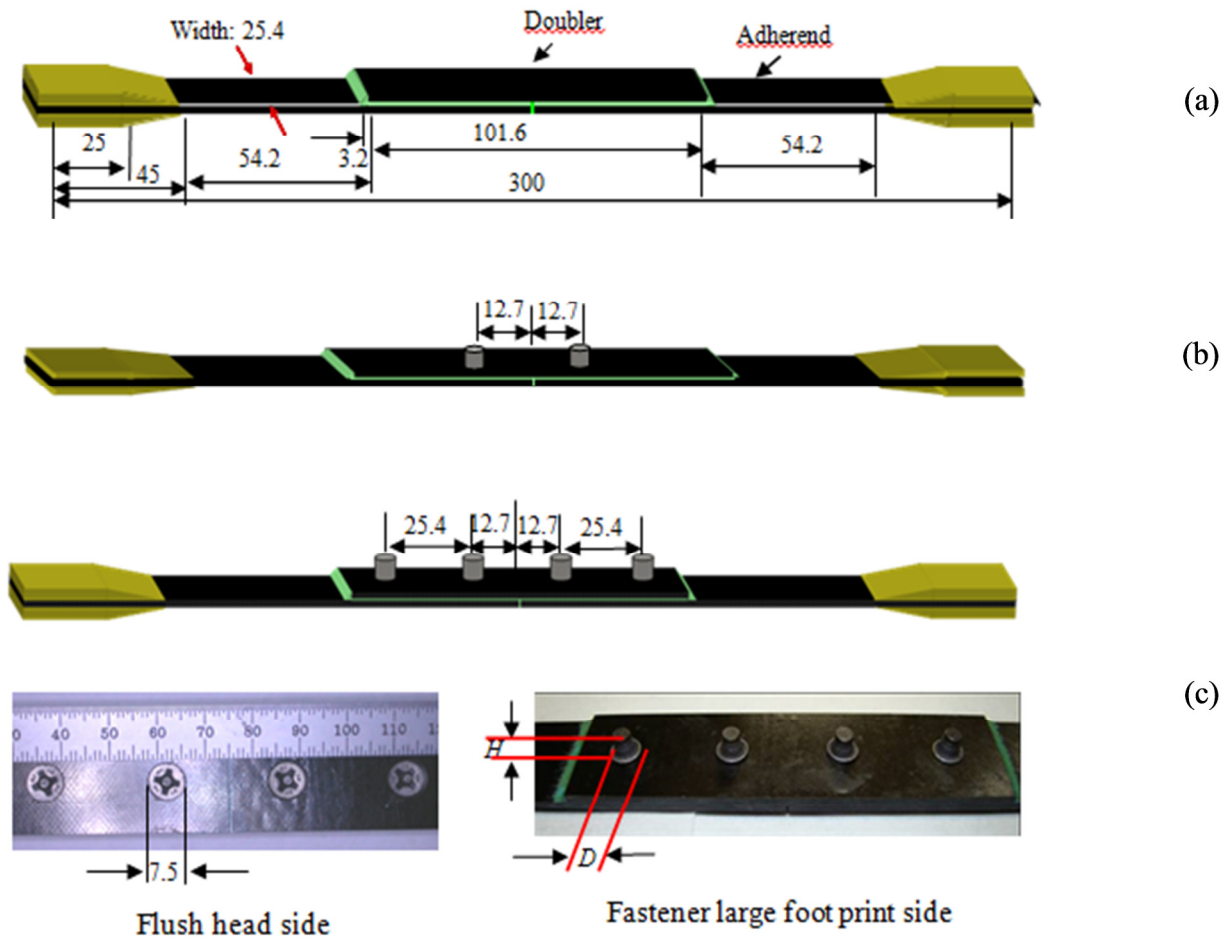


Figure 4.7 Schematic configuration of a composite butt joint configuration for (a) adhesively bonded joint, (b) BB1 joint with one-row fastener, (c) BB2 joint with two-row fasteners (not to scale, dimensions in mm).

Fatigue performance characterization of a composite butt joint configuration was studied. The study focused on failure mode, damage evolution and tensile stiffness degradation. Effects of surface ply orientation, doubler thickness, joint attachment and disbond on the joint fatigue performance were evaluated. The bonded-bolted joints with two-row fasteners installed in each overlap section had an extremely high fatigue performance, Figure 4.8. For such a bonded-bolted joint configuration with thick doubler, a minor disbond improved, rather than reduced, the joint fatigue performance. This outcome was examined using the corresponding joint tensile stiffness degradation curves, and a dominant failure mechanism was identified based on damage characteristics. The study showed that the butt joint made using appropriate elements, such as a thick doubler with two-row fasteners installed in each bonded overlap section, could have very good fatigue performance regardless of the presence of a minor disbond. An additional study identified that the degree of delamination, Figure 4.9, present in the doubler laminate could be the key mechanism dominating fatigue performance in the bonded-bolted joints.

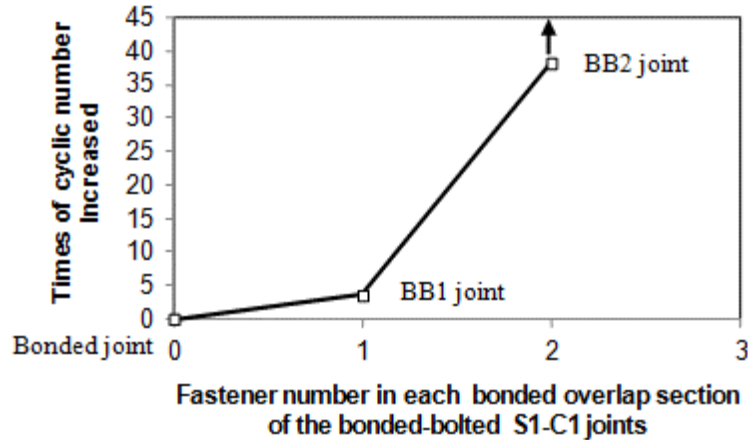


Figure 4.8 Effect of the fastener number on the fatigue life improvement for the bonded-bolted S1-C1 joints tested using the 100 MPa peak stress test condition.

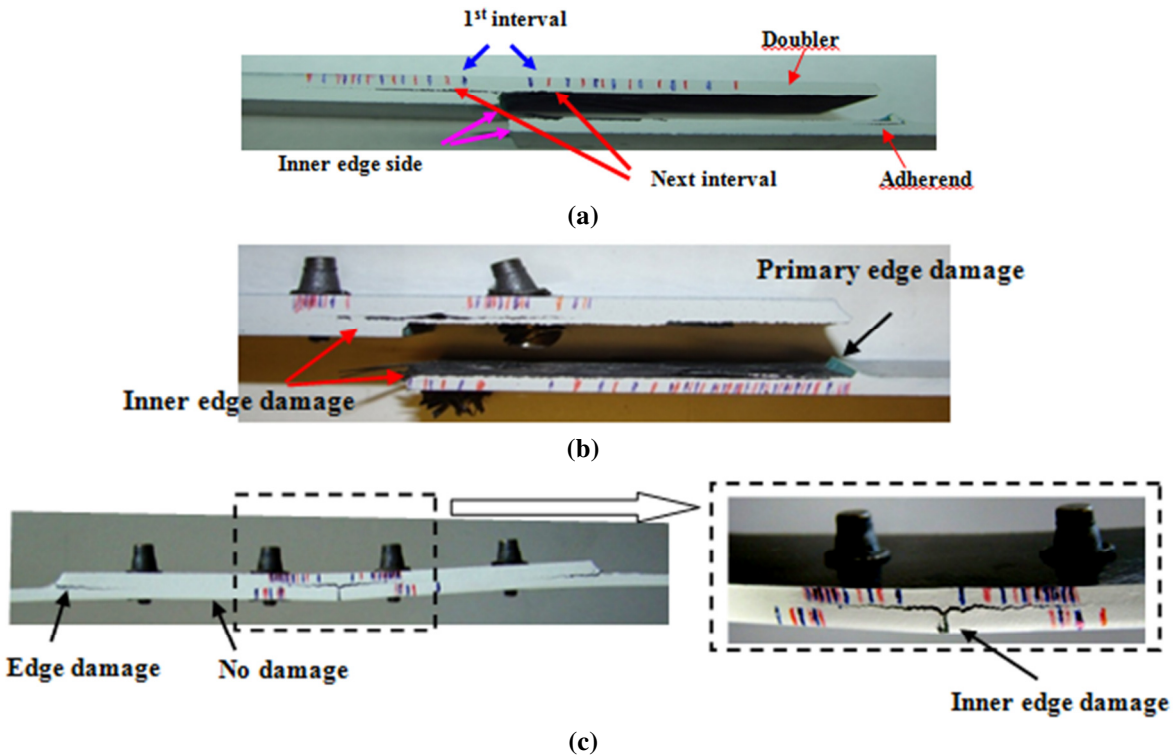


Figure 4.9 Damage tip detected for a (a) bonded, (b) BB1, and (c) BB2 case 1 joints during the tests

4.7.1 REFERENCE

- [1] G. Li, "Fatigue performance characterization of a composite butt joint configuration", Composites Part A, 51 (2013), 43-55.

4.8 MODELING OF PROGRESSIVE FAILURE IN BONDED COMPOSITE JOINT

G. Li and C. Li, NRC Aerospace

Application of cohesive zone (CZ) models to analyze the progressive failure of adhesively bonded laminated composite joints has been widely carried out. Studies showed that the shape of the traction-separation curves would have little impact on the numerical results of global load-

displacement response for the slender double cantilever beam (DCB) specimen, Figure 4.10. The bilinear traction law was found to be the simplest and most easy one to use. Open literature shows that three treatment methods have been used to introduce the CZ in the bonded joint failure simulation. An intuitive method is to replace the entire adhesive layer with a CZ, and where the zone thickness is the original adhesive thickness. The second treatment method is similar to the first one but the introduced CZ has a geometric zero-thickness to completely replace the original adhesive layer. The third method is to embed the geometrical zero-thickness zone along the adhesive mid-plane to form an “adherend + adhesive + CZ” (AACZ) system.

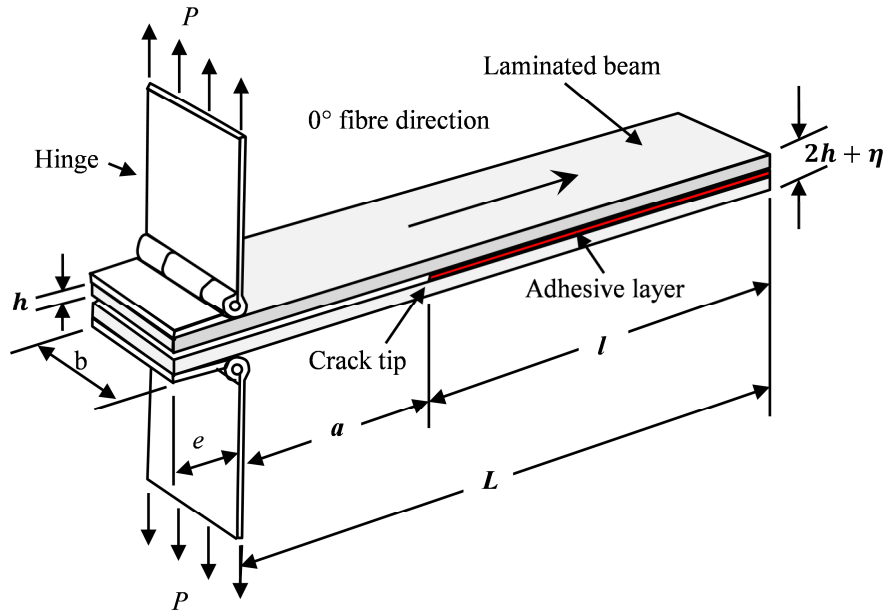
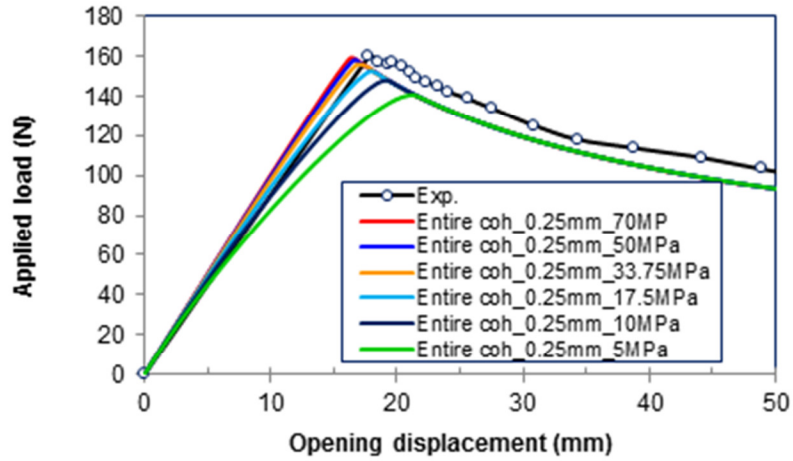
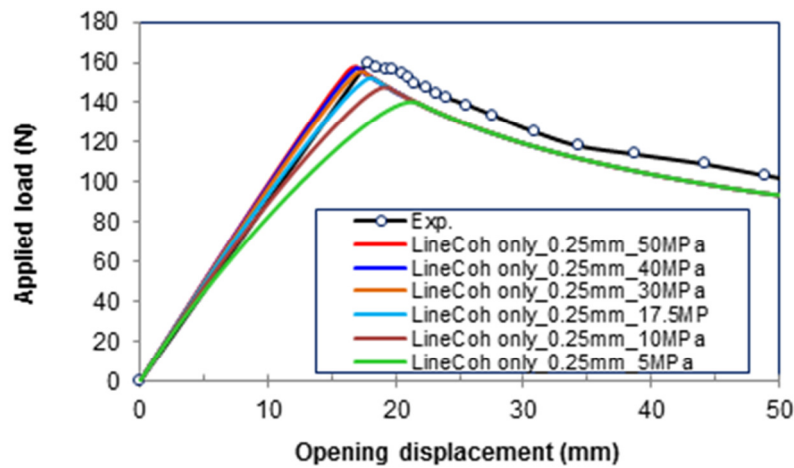


Figure 4.10 Laminated bonded DCB coupon and test setup

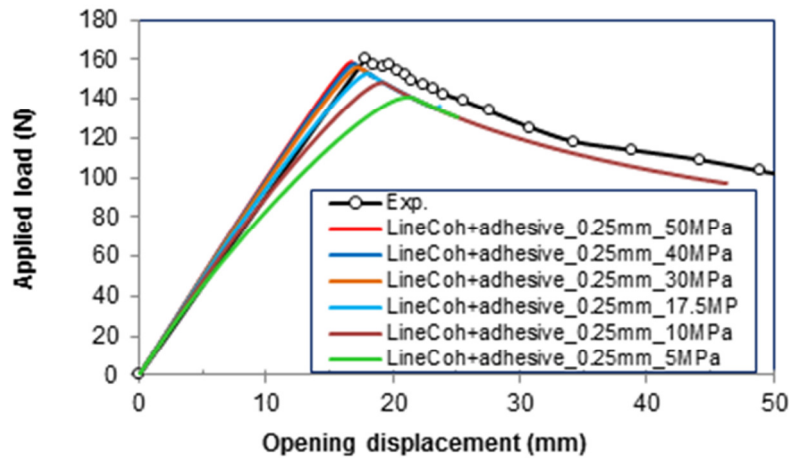
A comparison study of the three CZ treatments for the bonded joint failure simulation has been conducted recently by the authors. Responses to the global load-displacement, Figure 4.11 and local cohesive traction-separation were investigated in the simulation of progressive failure behaviour in a bonded double cantilever beam configuration. A remarkable finding was that the overall cohesive traction stiffness was much less than the assumed input value. In addition, the local nodal separation moment was identified. Consequently, the correct cohesive zone lengths were obtained using the extracted traction profile along the cohesive zone path at the corresponding moment. Information on the global load-displacement profile, traction stiffness, and cohesive zone length induced by the three zone cases were explored. The study explains why very small cohesive zone lengths were generated numerically, as compared to the proposed theoretical solutions. This study showed that ten or more elements were suggested to be placed along the cohesive zone length to practically simulate the experimental failure behaviour, Figure 4.12. The cohesive zone length should be estimated using the theoretical method with an interfacial strength obtained experimentally and an adjusted cohesive stiffness with three and/or four orders of magnitude less the original input one.



(a) Case 1



(b) Case 2



(c) Case 3

Figure 4.11 Comparison of the global load-displacement profile obtained from the experimental testing and the numerical analyses of (a) case 1, (b) case 2, and (c) case 3 models in the mesh 3 condition

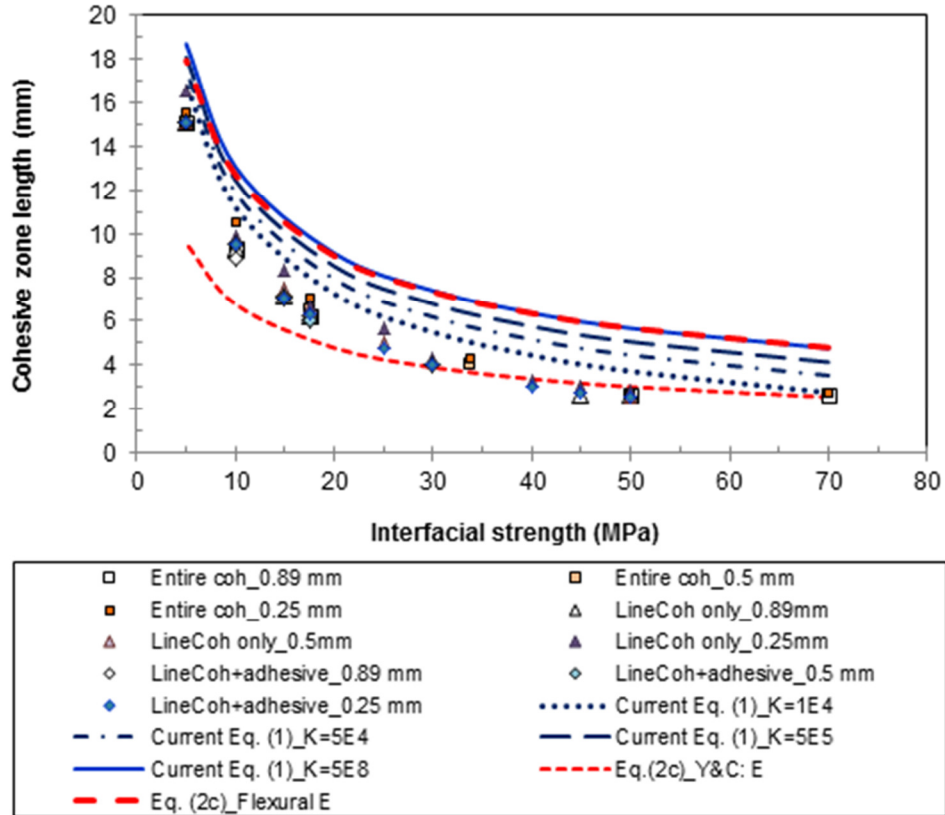


Figure 4.12 Comparison of the CZ lengths obtained from the numerical and theoretical results under the influence of the interfacial strength

4.8.1 REFERENCES

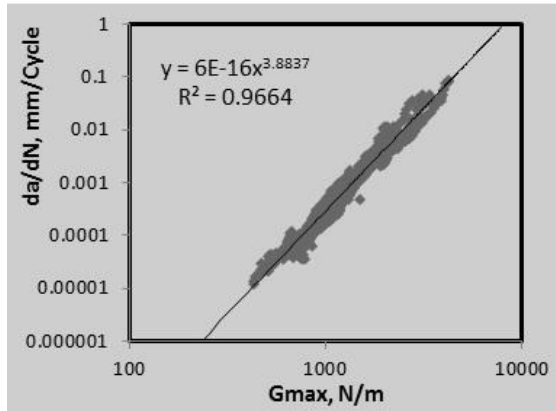
- [1] Li, G. and Li, C. (2015), "Assessment of debond simulation and cohesive zone length in a bonded composite joint", *Composites: Part B*, 69, pp. 359-368

4.9 LONG-TERM DURABILITY OF ADHESIVELY BONDED COMPOSITE JOINTS UNDER STATIC AND FATIGUE LOADING*

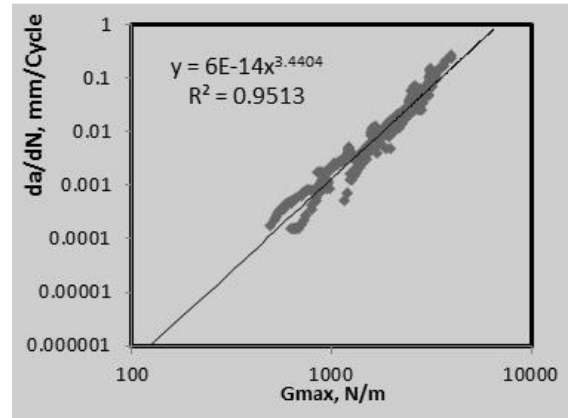
C. Li, NRC Aerospace

*Paper being presented at ICAF2015

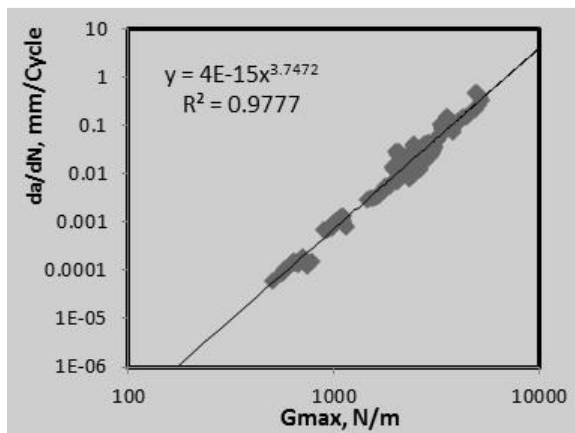
The 21st century marks an era where ultra-high specific strength and stiffness carbon-fibre reinforced composite materials are increasingly used for fabricating aircraft structures. It is well known that composite materials are susceptible to environmental degradation, which is of particular concern for adhesively bonded composite joints due to the lack of non-destructive methods to detect damage for the quantitative assessment of bond strength. Experience has indicated that a better understanding of fatigue issues within composites is important not only for risk analysis of structures that may be subjected to undetectable incidental and environmental damages but also allows for life extension programs and more efficient design of composites.



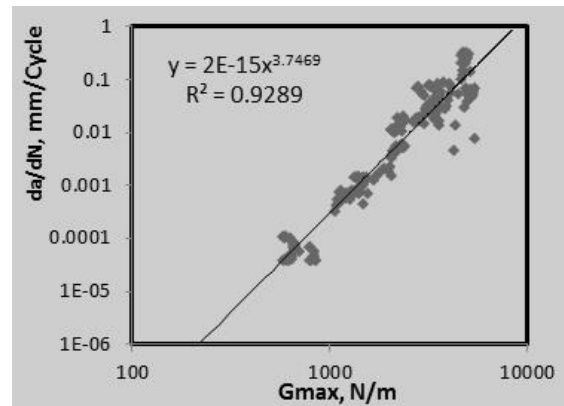
(a) Power Law Applied to Disbond Growth at
 $G_{II}/G_T = 0.2$



(b) Power Law Applied to Disbond Growth at
 $G_{II}/G_T = 0.4$



(c) Power Law Applied to Disbond Growth at
 $G_{II}/G_T = 0.6$



(d) Power Law Applied to Disbond Growth at
 $G_{II}/G_T = 0.8$

Figure 4.13 Power law fits applied to disbond growth data for RTA condition

In this past year, National Research Council focused its research effort on testing and modeling static and fatigue performance of bonded composite joints under Mixed Mode I/II loading. Strain energy release rates under mixities (G_{II}/G) of 0, 0.2, 0.4, 0.6 and 0.8 was investigated. The quasi-static test results show that the total fracture toughness value increases with the mode mixity, as bonded joints have more resistance towards in-plane shear. The coefficient of variation also increases with greater Mode II contribution, indicating increasing instability of disbond growth and associated greater uncertainty under Mode II. Fatigue damage growth in a full range of mode mixtures was also investigated, as shown in Figure 4.13. It was found that there was no clear identifiable pattern that governs the relationship between the fitted constants in Paris Law relationship (as shown on each graph), and the mode mixtures. Thus, alternative interpretations of the experimental results were explored in this study. As shown in Figure 4.14, a fit to Kenane and Benzeggagh equation was found to provide better illustration than other existing models of disbond growth with strain energy release for the range of the load mixity, although the R-square value of 0.8 is still quite low. Post-test of fracture failure analysis shows a progressive change in failure modes from pure cohesion failure (failure at the bond interface) at low mixity, to a combined cohesive/substrate failure, which suggest that the failure modes be

taken into account in developing models for load mixity effect on delamination/disbond growth of a bonded composite joints.

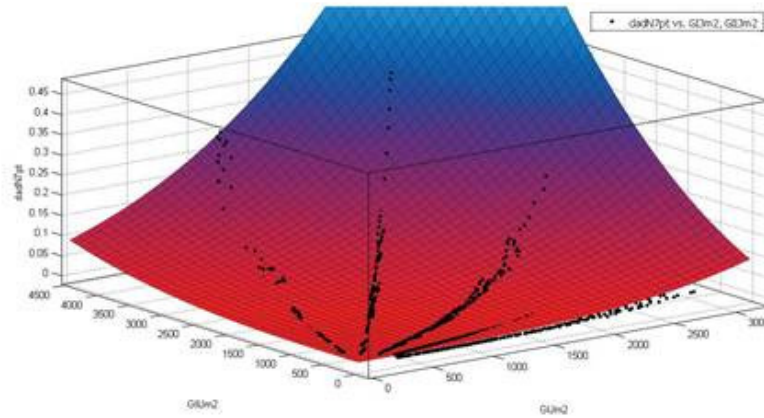


Figure 4.14 A 3-D fit of delamination/disbond growth rate of a bonded composite joints to Kenane and Benzeggagh Equation

Further studies of environmental effects on disbond growth of bonded composite joints under static and fatigue loading were also conducted. The conditioned specimens exhibited a significant reduction in fracture toughness G_c at up to 50%, demonstrating the significant effect of environmental ageing. Such effect was also apparent on fatigue disbond growth rates for the laminates and environmental aged joints, where typically a faster rate was observed as compared to behavior of the unconditioned ones, as shown in Figure 4.15. Subsequent analysis of the failure surfaces revealed a change in failure mode of the specimens subjected to long-term environmental exposure that could partially explain the change in static and fatigue delamination and disbond performance of the laminates and adhesively bonded composite joints.

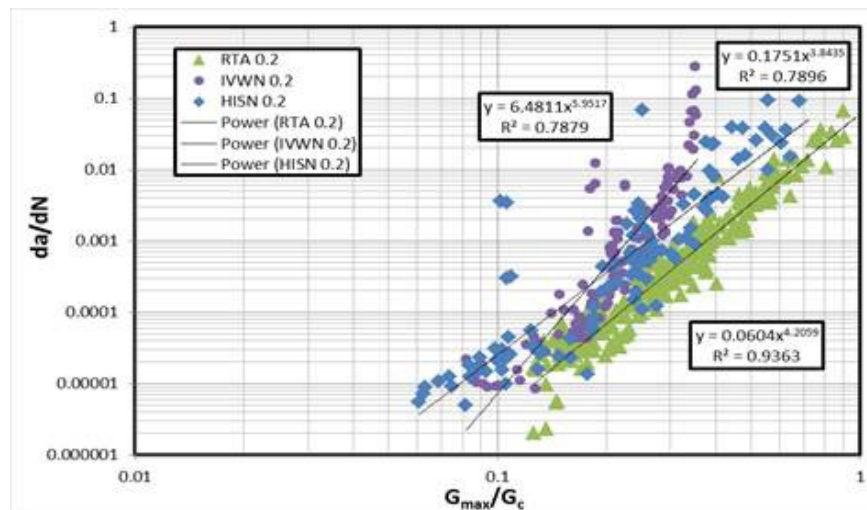


Figure 4.15 Comparison between environmental conditions (RTA – room temperature ambient, IVWN-70°C vapor; HISN- 82°C salt water immersion) for mode mixture = 0.2

5.0 FRACTURE MECHANICS AND CRACK PROPAGATION STUDIES

5.1 A MECHANISM-BASED APPROACH TO CREEP, LOW CYCLE FATIGUE AND THERMOMECHANICAL FATIGUE LIFE PREDICTION

X.J. Wu, NRC Aerospace

Based on the premise of deformation mechanism map as initially proposed by Ashby, NRC has developed a mechanism-based approach to creep, low cycle fatigue (LCF) and thermomechanical fatigue (TMF) life prediction—the integrated creep-fatigue theory (ICFT). In this theoretical framework, the total strain is formulated as the summation of rate-independent plasticity and creep strains:

$$\varepsilon = \left(\frac{\sigma}{E} + \varepsilon_p \right) + \varepsilon_{gbs} + \varepsilon_g \quad (1)$$

where ε is the total strain, σ is the stress, E is the elastic modulus, ε_p is the rate-independent plastic strain, ε_{gbs} is grain boundary sliding (GBS) strain, ε_g is intragranular deformation (ID). The participation of each microscopic deformation mechanism is included via the constitutive law for the respective deformation mechanism.

Second, a holistic damage equation is derived based on the damage accumulation process that consists of nucleation and propagation of surface/subsurface cracks in coalescence with internally distributed damage/discontinuities:

$$\frac{1}{N} = \left(1 + \frac{l}{\lambda} \right) \left\{ \frac{1}{N_f} + \frac{h}{a_c} \right\} \quad (2)$$

where N_f is the pure mechanical fatigue life limited by rate-independent plasticity (ε_p) via Coffin-Manson relationship, l is the size of internally distributed micro-cracks and λ is their inter-spacing, h is the newly formed oxide scale thickness in every cycle, and the critical crack length a_c is given by the well-known fracture mechanics concept:

$$a_c = \frac{1}{\pi} \left(\frac{K_{IC}}{Y\sigma_{\max}} \right)^2 \quad (3)$$

When the material creeps alone, its strain vs. time behaviour is described by Eq. (1), which includes the primary, secondary and tertiary stages, and the creep life is limited by the competition of intragranular deformation (ε_g) and grain boundary sliding (ε_{gbs}), reaching either the grain ductility or a critical GBS level, whichever comes first.

Under alternating load and/or temperature conditions, which result in LCF/TMF. The cyclic stress-strain response and/or hysteresis behaviour is described by Eq. (1) with the involvement of all possible deformation mechanisms. In this case, fatigue and corrosion/oxidation is responsible for surface crack nucleation and propagation, and creep and/or intergranular embrittlement contributes to internally distributed damage. As formulated in Eq. (2), the total LCF/TMF life is

then limited by mechanical fatigue and corrosion/oxidation compounded with the internal damage of the material. Eq. (1) and (2) also predict the failure mode, as it delineates the contribution of each deformation/damage mechanism and recognizes the dominant one in quantitative terms.

The ICFT has been shown to successfully describe the many facets of high temperature deformation and life behaviours, including effects of strain range and strain rate, minimum and maximum temperature and hold time during TMF loading, etc. for Ni and Co base superalloys and ductile cast irons as reported in the following publications.

5.1.1 REFERENCES

- [1] X.J. Wu, An Integrated Creep-Fatigue Theory for Material Damage Modelling, Key Engineering Materials Vol. 627 (2015) pp 341-344.
- [2] X.J. Wu, T. Quan, R. MacNeil, Z. Zhang and C. Sloss, Failure Mechanisms and Damage Model of Ductile Cast Iron under Low-Cycle Fatigue Conditions, Metall. and Mater. Trans. A, vol. 45A (2014) pp.5088-5097.
- [3] X.J. Wu, T. Quan, R. MacNeil, Z. Zhang, Xiaoyang Liu and C. Sloss, Thermomechanical Fatigue of Ductile Cast Iron and Its Life Prediction, Metall. and Mater. Trans. A (2015), accepted.
- [4] X.J. Wu and Z. Zhang, A Mechanism-Based Approach from Low Cycle Fatigue to Thermomechanical Fatigue Life Prediction, Proceedings of ASME Turbo Expo 2015, June 15–19, 2015, Montréal, Canada, paper# GT2015-43974.

5.2 APPLICATION OF EXPERIMENTAL MECHANICS TECHNIQUES FOR BIAXIAL FATIGUE TESTING

D. Backman and M. Liao, National Research Council Canada

The National Research Council Canada (NRC) has recently upgraded their planar biaxial test frame. The upgrade, which involved the addition of a new control system as well as the installation of actuator supports, has resulted in a significant performance increase for Canada's largest planar biaxial test frame. The planar biaxial test frame now has the capability to operate at 22 kN [50 kips] and at frequencies of 5 Hertz or higher.

The newly commissioned planar biaxial test frame has been set up to take advantage of NRC's capabilities in experimental mechanics. Deploying advanced experimental mechanics techniques to biaxial fatigue testing for cruciform specimen design, testing machine calibration, and fatigue crack nucleation/growth monitoring. NRC currently operates a suite of advanced experimental mechanics techniques including Digital Image Correlation (DIC), automated Photoelasticity, and Thermoelastic Stress Analysis (TSA). In a recent joint effort with an external client, DIC techniques have been used for developing a cruciform specimen (smooth and notched), together with finite element modeling (FEM) that was carried out by the client. For the biaxial testing, the DIC results are used to examine the alignment of the test machine. During testing, a combination of DIC and TSA were proposed to record, display and analyze results, aiming to detect and

monitor crack nucleation and growth. A comparison between the strains measured with DIC and the numerical solution are shown in Figure 5.1.

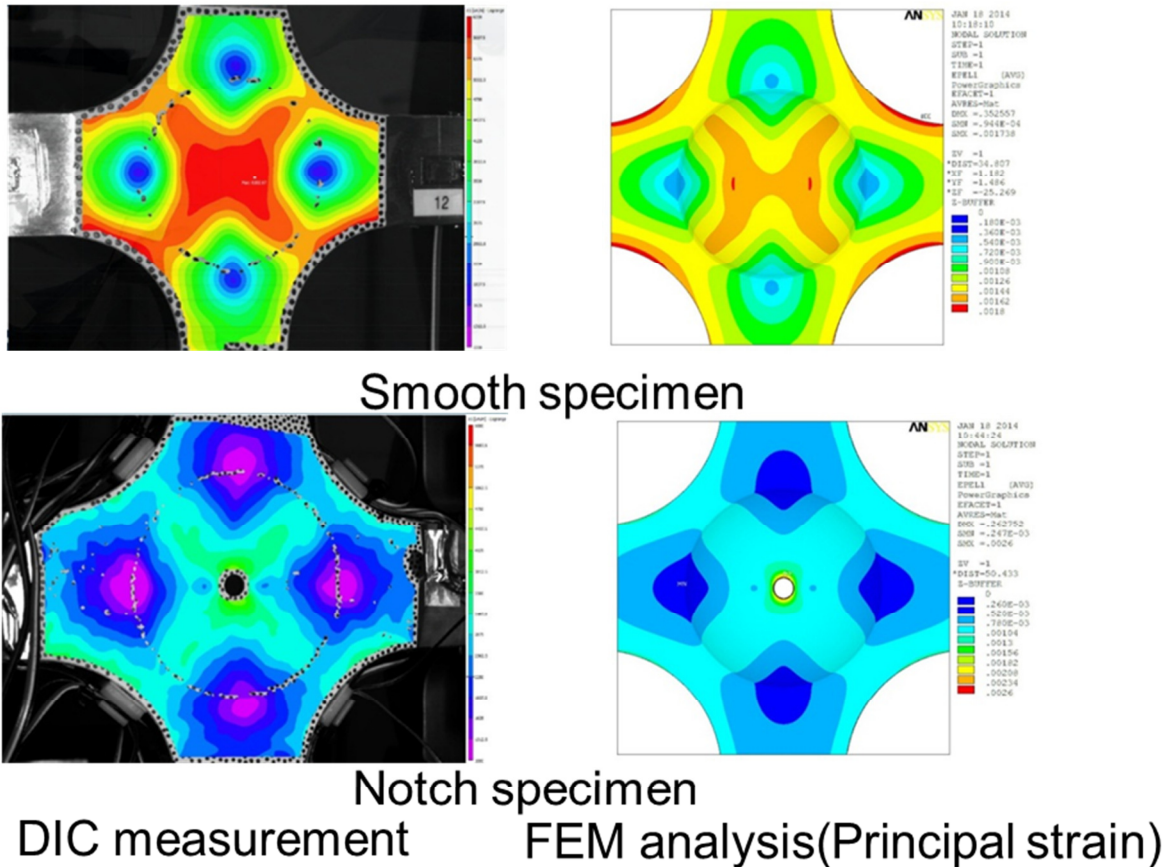


Figure 5.1 Comparison of DIC and FEM analysis for a cruciform specimen

5.3 QUANTITATIVE FATIGUE DAMAGE MEASUREMENTS IN CARBON FIBRE REINFORCED POLYMERS

J. Laliberté and N. ElAgamy, Department of Mechanical and Aerospace Engineering, Carleton University

Research Objectives

- ✓ Aided by non-destructive high resolution micro-CT Skyscan 1173, work aimed to carry out a phenomenological study on fatigue behaviour in CFRP cross-ply laminates subjected to monotonic cyclic loading, experienced by typical modern aircraft structures during flight.
- ✓ Statistically analyze the quantitative data traced on geometry and locations of propagated cracks relative to the life cycle to obtain fatigue crack growth rates in the 3 orthogonal planes.
- ✓ Strain energy release rates, G , can hence be calculated by using available laws.
- ✓ Using the G_I , G_{II} and G_{III} values to define cohesive zone model (CZM) parameters for the 3 damage modes; opening, in-plane shear and out-of-plane shear.
- ✓ The sought information will be mathematically implemented in a user sub-routine written for the ABAQUS finite element analysis tool to simulate the evolution and propagation of high-cycle fatigue loading.

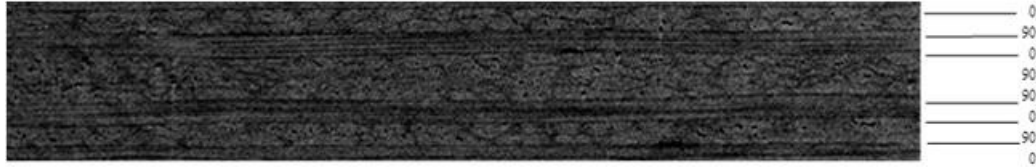


Figure 5.2 Virtual cross-section of the sample in X-Y (transverse) plane clearly identifying the 0/90 layers

Notable Progress

- ✓ Micro-CT scans acquired so far provided a qualitative assessment of fatigue damage types, scenario of their interactions and sequence of occurrence.

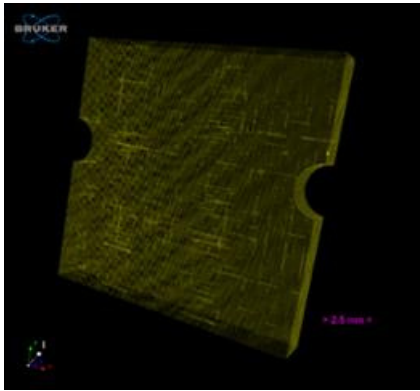


Figure 5.3 3D reconstructed rendered volume of 1905 rotational scans provided by microCT. Opacity level was adjusted to visualize defects

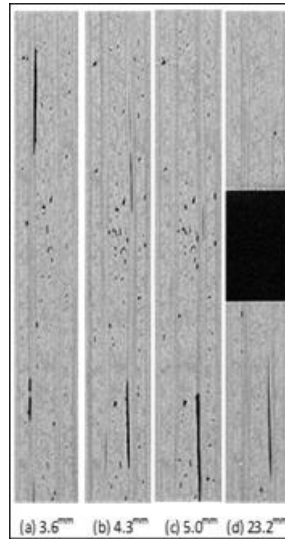


Figure 5.4 Virtual cross-sections of the sample at multiple positions throughout the thickness clearly identifying cracks

- ✓ A procedure was set for testing the functionality of available tools in terms of virtual slicing, segmentation, 3D plotting and statistical analysis and ABAQUS implementation.
- ✓ Fatigue crack growth rates, da/dn were obtained for each plane, which were interpreted in terms of the 3 damage modes; opening (mode I), in-plane shear (mode II) and out-of-plane shear (mode III). By applying linear elastic fracture mechanics (LEFM) laws, strain energy release rates were calculated.

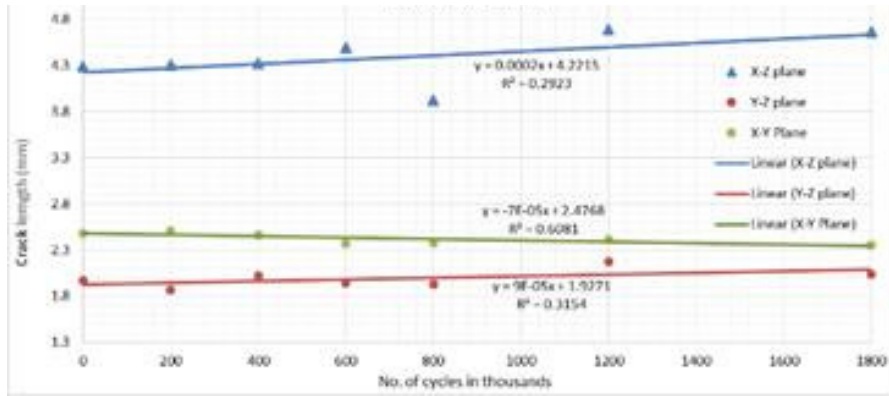


Figure 5.5 da/dn in 3 planes

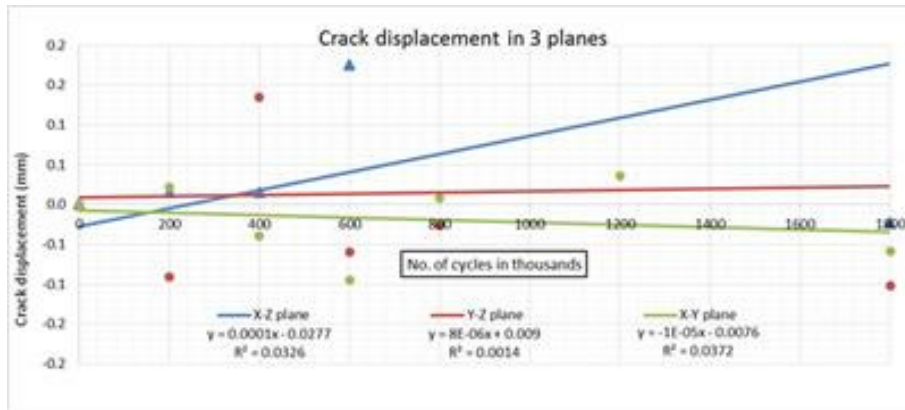


Figure 5.6 Crack displacement in 3-planes

- ✓ Considering a bi-linear triangular CZM curve, determining 2 parameters led to identifying the coordinates of the triangular curve for each of the 3 modes. The known variables were the area under each curve, namely the fracture energy (strain energy release rate) and the other variable was the slopes of linearly ascending traction-separation zones, physically interpreted as the moduli of elasticity, E_{11} , E_{22} and E_{33} . Maximum traction and maximum separation were calculated for each of the 3 damage modes, differentiating between modes II and III in a novel manner.

Table 5.1 Material Properties

Orthogonal Planes	X-Z plane	Y-Z plane	X-Y plane
	Opening mode (Mode I fracture)	In-plane shear mode (Mode II fracture)	Out-of-plane shear (Mode III fracture)
VOI slice area (pixels X pixels)	1972 x 1370	224 x 1370	1972 x 224
VOI slice area (mmXmm)	23.82 x 16.55	2.71 x 16.55	23.82 x 2.71
Number of slices	224	1972	1370
Plane thickness (mm)	2.71	23.82	16.55
Threshold method	Minimum	Triangle	Triangle
Total number of detected cracks	26	30	40
area of initial detected voids (pixel ²)	5.0353E+05	2.3215E+05	6.1600E+05
% area of initial detected voids	0.0832%	0.0389%	0.1018%
area of voids after 1.8x10 ⁶ fatigue cycles (pixel ²)	5.1335E+05	1.8974E+05	5.4448E+05
% area of voids after 1.8x10 ⁶ fatigue cycles	0.0848%	0.0314%	0.0900%
% change in void content	1.9202%	-19.4911%	-11.6204%
Average initial crack length (mm)	2.1180	1.7527	1.8744
Average final crack length (mm)	2.1457	1.7105	1.7400
Observed da/dn slope	1.9940E-04	9.0000E-05	7.0000E-05
Paris law using Blanco's constants	$da/dn = 2.1 G_I^{5.09}$	$da/dn = 0.12 G_{II}^{4.38}$	$da/dn = 0.12 G_{III}^{4.38}$
Strain energy release rate $G_{I,II,III}$ (N/mm)	0.16208	0.19344	0.18265
Modulus of Elasticity (MPa)	E ₁₁ =120,000	E ₂₂ =10,500	E ₃₃ =10,500
Maximum CZM displacement (mm)	0.0520	0.1920	0.1865
Maximum CZM traction (N)	6.2369	2.0155	1.9585

5.3.1 REFERENCES

- [1] N. ElAgamy, J. Laliberté and F. Gaidies (2015). Quantitative Analysis of fatigue cracks in laminated CFRP composites using micro-computed tomography. Manuscript in preparation.
- [2] N. ElAgamy, C. Martin, T. Sachdeva and J. Laliberté (2014). Proposed procedure to simulate 3D multi-mode fatigue behaviour in laminated CFRP using micro-CT scans in ABAQUS. In: CAMX conference (The Composites and Advanced Materials Expo), Orlando FL, USA, October 12-16, 2014.
- [3] N. ElAgamy and J. Laliberté (2014). Historical development of geometrical modelling of textiles reinforcements for polymer composites: a review, Journal of Industrial Textiles, First publication on October 20, 2014, DOI:10.1177/1528083714555781.
- [4] N. ElAgamy, J. Laliberté, F. Gaidies and J. Goldak (2014). Qualitative characterization of fatigue damage propagation in laminated carbon fibre reinforced polymers by using micro-computed tomography. In: SAMPE conference (Society for Advanced Materials and Process Engineering), Seattle, WA, USA, June 2-6, 2014

5.4 TENSILE FATIGUE BEHAVIOUR OF TAPERED GLASS FIBRE REINFORCED EPOXY COMPOSITES CONTAINING NANOCCLAY

S. Helmy and S.V. Hoa, Department of Mechanical and Industrial Engineering, Concordia University

In the past few decades, composite materials have been used in more and more applications. This is more pronounced where reducing the structure non-useful weight becomes a crucial design criterion so as to maximize the weight of the useful payload of such structures. Examples of these applications include wings and fins of aircrafts, helicopter yoke and blades, robot arms, and

satellites. In addition to removing unnecessary weights, tapering the structure, i.e., varying its thickness from one point to another is, in some applications, a design requirement to allow flexibility. One example of tapered designs is the flexbeam of the helicopter main rotor yoke. Material thickness variations are required to optimize the design of laminated composite structures. These thickness variations are accomplished by dropping layers of material (plies) along the structure to match the load carrying requirements.

The use of nanocomposites stems from that fact that interphase (properties different from the constituent materials) with a considerable thickness is considered as a source of energy dissipation in composite structures. Another source of energy dissipation related to interphase is due to the friction and slippage of unbound region or delaminated area of clay platelet and matrix. As a consequence, it can be expected that adding nano-particles (e.g. nano-clay) in polymer matrix would improve the ability of energy dissipation under dynamic loading thus enhancing the damping property.

Tapered specimens were composed of three sublaminates: one internally dropped sublaminates, and two outer continuous sublaminates (belt sublaminates) that cover the dropped sublaminates. All of the laminates investigated were symmetric. The laminates were tapered from 40 plies to 32 plies through a taper angle of approximately 10° . The dropped sublaminates contains 8 plies and terminates at the midplane of the laminates. The laminates were fabricated from the following materials; Unidirectional S-glass fibres manufactured by AGY World Headquarters and supplied by Aerospace Composites Products Inc, Organoclay Nanomer I.30E supplied from Nanocor Inc and the resin and hardener were EPON 828 and EPICURE 3046, respectively, both supplied by Hexion Specialty Chemicals. A high-speed stirring method was used to disperse the clay in resin.

Tension tests were conducted prior to fatigue testing using a digitally controlled (MTS) Servo Hydraulic Testing Machine at a crosshead rate of 2 mm/min. Tensile strength was calculated by dividing the maximum load over the cross-sectional area of the thin part of the tapered specimen. The results showed only a small influence of the nanoclay filler on the stiffness which appeared to promote a more brittle-like behavior that led to a lower strain at failure. The fatigue testing of the specimen was conducted in force-controlled mode. All fatigue tests were carried out under a load ratio ($\sigma_{\min}/\sigma_{\max}$) of $R=0.1$ and at a frequency lower than 10 Hz to avoid temperature rise especially at high stress levels. Three specimens were tested at each stress level namely, 0.8, 0.6, 0.5, and 0.35 S_{ut} . Development of damage during the tests was observed and monitored using a long-distance Questar QMI (Maksutov-Cassegrain Catadioptric) telescope manufactured by Questar Corporation. The light source (lamps) was placed on the side opposite to the strain gauge to minimize the thermal effects on the strain gauge. More importantly, the position of the light source was properly adjusted to maximize the shade contrast inside the specimen for a clearer crack progress monitoring. Specimen monitoring was focused at the edges. Any damage to the specimen edges was easily recognized as bright areas on the surface. In some cases when a “noise” (indicating the occurrence of cracking within the laminate) was reported, the experiment was stopped for observation. The experiment was then continued until the specimen failed completely.

Figure 5.7 shows the fatigue behaviour of the three stacking configurations for both filled and unfilled laminates. This figure shows that, for the same level of maximum applied stress, laminates with nanoclay exhibit longer fatigue life than laminates without. It also shows that as far as fatigue life improvement is concerned, nanoclay modification is more effective at the low stress levels (or high cycle regime) and less effective at high stress levels. At these high levels, nanoparticles are less resistive in suppressing crack propagation.

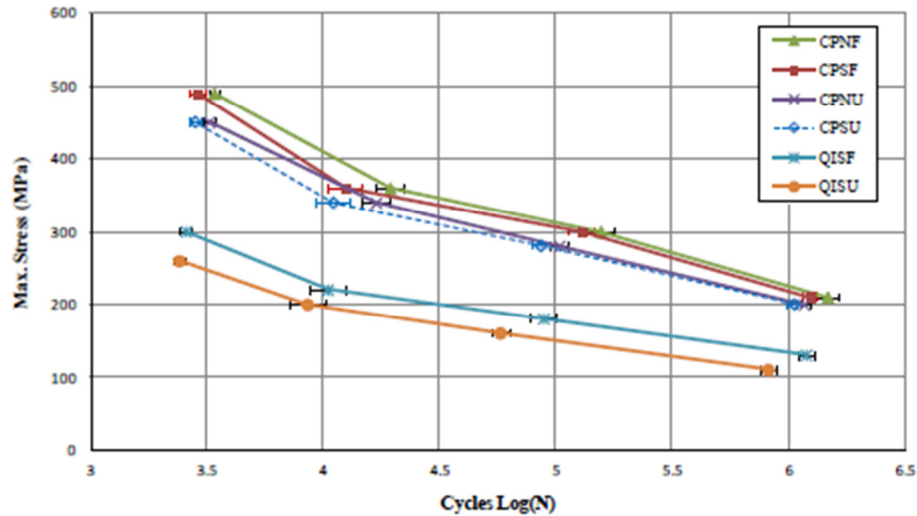


Figure 5.7 Tensile fatigue strength, S-N curves, for all specimens

The results of a study of tensile fatigue in glass/epoxy tapered beam composites with different stacking sequences, where nanoclay had been incorporated in the matrix can be summarized as:

1. The static tensile strength and modulus of glass/epoxy tapered composites are slightly enhanced by the addition of nanoclay. The presence of nanoclay in the matrix increases the ultimate strength and decreases the strain to failure.
2. According to the failure criterion adopted, i.e. total separation of the specimens, tensile fatigue life was significantly extended with the incorporation of nanoclay to glass/epoxy tapered beam. The maximum improvement was about 54% with quasi isotropic laminates.
3. Nanoclay suppresses the fatigue damage growth in terms of damage index and crack growth rate over the whole fatigue life except the early stage of loading.

5.5 BENCHMARK ASSESSMENT ON FATIGUE PROPAGATION IN A BONDED COMPOSITE JOINT STRUCTURE

G. Li and C. Li, NRC Aerospace

To date, propagation simulations of debonds under static and fatigue loadings via virtual crack closure technique (VCCT) using a commercial FE code have not been widely reported in the open literature. The benchmark examples reported thus far by Krueger (2008 and 2010) and Orific and Krueger (2010 and 2012) are only for laminates with small G_{IC} values. Therefore, there is a need for benchmark examples for high G_{IC} in bonded composite joints. In addition, the

effects of load ratio need to be investigated. This study is important for the development of reliable and affordable numerical methods to predict the strength and fatigue performance of large laminated and/or bonded composite structures used in aircraft.

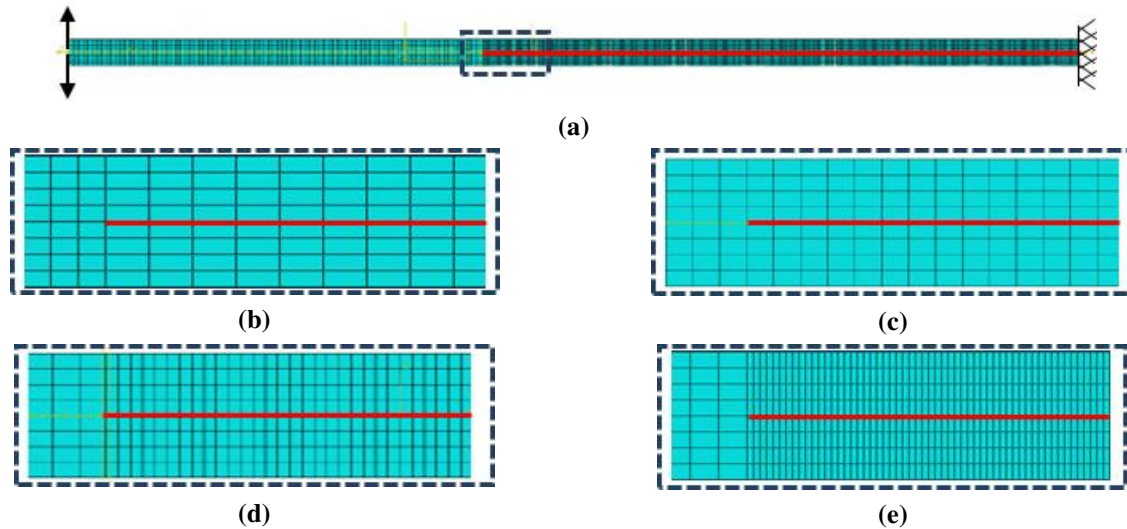


Figure 5.8 Schematics of (a) an overall DCB FE model with 0.5 mm long elements in the debonded region (12.7mm in length) and the bonded region meshed using either (b) 0.87 mm, (c) 0.5 mm, (d) 0.25 mm, or (e) 0.125 mm long elements for assessing sensitivity with respect to element size

Progressive failure and fatigue debond propagation in a mode I bonded composite double cantilever beam were analyzed using two-dimensional finite element methods and the virtual crack closure technique (VCCT), Figure 5.8. Four mesh densities were assessed in the static progressive failure simulation. Analyses using the shortest 0.125 mm long elements terminated prematurely for a wide range of critical strain energy release rates G_{IC} (0.295, 0.6, 2.95, and 4 N/mm). The FE models with the other three meshes resulted in good agreement with the experimental load versus opening displacement curve. These three meshes were then used in the performance assessment of the debond propagation simulation. The fine mesh models, especially with the 0.25 mm long elements, gave a higher propagation rate, da/dN , than the coarse mesh models, and this difference increased with increasing load ratio ($R = 0.1, 0.3, 0.5,$ and 0.7 at 1 Hz frequency). The benchmark example seems to be applicable only for the $R=0.1$ condition based on the agreement between the FE simulations and the experimental results in both da/dN (debond fatigue propagation rate) and $a - N$ (debond length vs cycle), Figure 5.9.

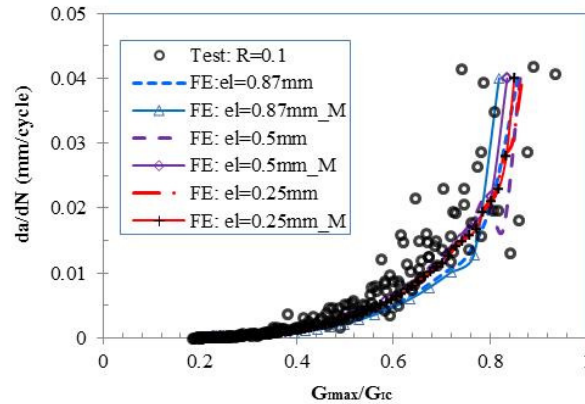


Figure 5.9 Comparison of the debond fatigue propagation rate versus normalized G_{\max} profiles obtained from experimental and numerical results for the $R = 0.1$ testing condition, where “*_M” refers to the $c_1 = 0$ condition reflecting an assumed immediately stable fatigue propagation

5.5.1 REFERENCES

- [1] G. Li, C. Li (2014), “Effect of R -Ratio on Simulation Performance of Fatigue Debond Propagation in Laminated Composite Structure”, in Proceedings of American Society for Composites 29th Technical Conference, University of California San Diego, La Jolla, CA USA, September 8-10, 2014.
- [2] G. Li, C. Li (2014), “Simulation of progressive debond and fatigue growth in a laminated composite structure using VCCT”, LTR-SMM-2014-0076, NRC Aerospace.

5.6 NUMERICAL PREDICTIONS OF EVOLVING CRACK FRONT GEOMETRY AND FATIGUE LIFE FROM STRAIGHT AND COUNTERSUNK HOLES IN THIN PLATES

D. Wowk, Royal Military College of Canada

When performing fatigue life predictions using linear elastic fracture mechanics, the shape of the crack front must be assumed. For example, the crack front geometry for corner cracks emanating from straight holes or countersunk holes in thin plates is typically represented by an ellipse. When the component of interest has complex geometry or loading, it is difficult to make an assumption with regards to crack front shape. It was therefore deemed necessary to develop a program to predict fatigue life that does not rely on an assumed crack front geometry. Rather, the crack front shape is determined iteratively using 3D finite element simulations as the crack propagates. Version 1.0 of a program, called the ACGP (Automatic Crack Growth Program) has been completed by Lucas Alousis as part of his Master’s thesis [1], and has the capability of predicting the fatigue life and crack front shape for five different geometric configurations.

Program Description

The ACGP uses linear elastic fracture mechanics along with 3D finite element simulations to predict the shape of an evolving crack front and fatigue life for corner cracks in thin plates. The commercial finite element package, Stresscheck is linked with Excel spreadsheets using Com API. The crack itself is assumed to be planar, and is represented by a spline curve instead of the often assumed ellipse, which allows for complex crack front geometries to be represented. Five

separate modules have been developed for the following cases (Figure 5.10): Version 1-corner crack at a hole, Version 2-corner crack at a notch, Versions 3 to 5-cracks from the bore, knee and upper surface of a countersunk hole.

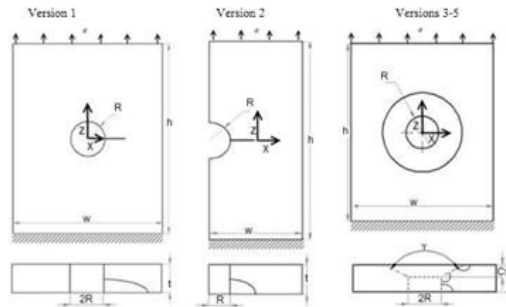
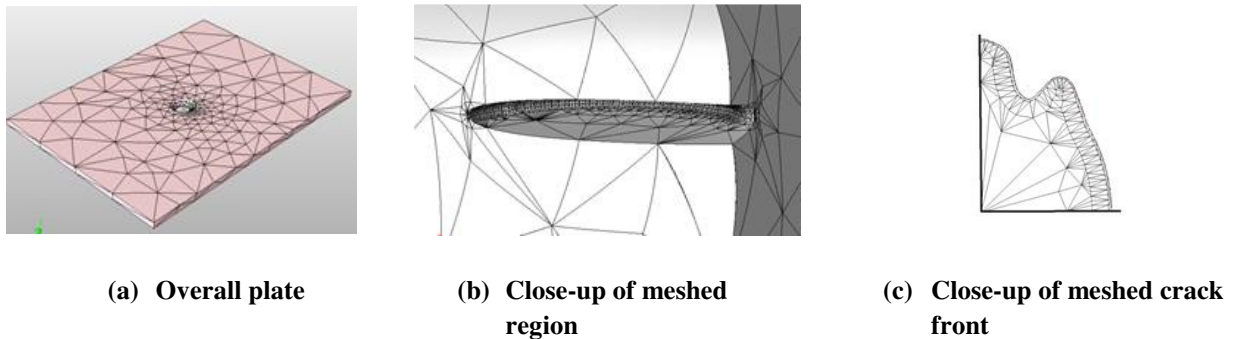


Figure 5.10 The five cases supported by the ACGP: a) Version 1-corner crack at a hole, b) Version 2-corner crack at a notch, c) Versions 3 to 5-cracks from the bore, knee and upper surface of a countersunk hole.

The core of the program consists of automatically generated 3D finite element simulations, where the geometry of the crack itself is explicitly defined using spline points (Figure 5.11). The stress intensity factors (K) are extracted at multiple locations along the crack front and the Paris Law is then used to determine the crack growth increment for each point along the crack front (Figure 5.12). The new crack shape is input back into the finite element software and a new simulation is run. Iterations continue until the crack grows to a user-specified length. The program will output the fatigue life along with plots of the shape of the crack front.

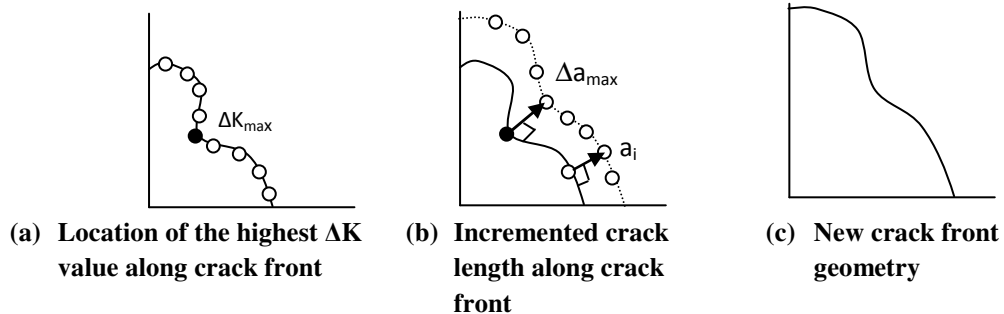


(a) Overall plate

(b) Close-up of meshed region

(c) Close-up of meshed crack front

Figure 5.11 Examples of automated finite element simulations



(a) Location of the highest ΔK value along crack front

(b) Incremented crack length along crack front

(c) New crack front geometry

Figure 5.12 Crack growth process

Verification and Results

The predicted crack shape was compared to experimental test results provided by NRC [2], from a single edged notch tension (SENT) coupon machined from an aluminum 7075-T73 forging. Figure 5.13a shows the predicted shape of the crack front using the ACGP (red) compared to the experimentally measure shape (blue). The geometry is predicted within a maximum of 5% difference at the intersection with the notch. The predicted crack shape was also compared to results produced by AFGROW for countersunk holes. Figure 5.13b shows that other than at the transition from corner crack to knee crack, the crack front geometry is predicted quite well.

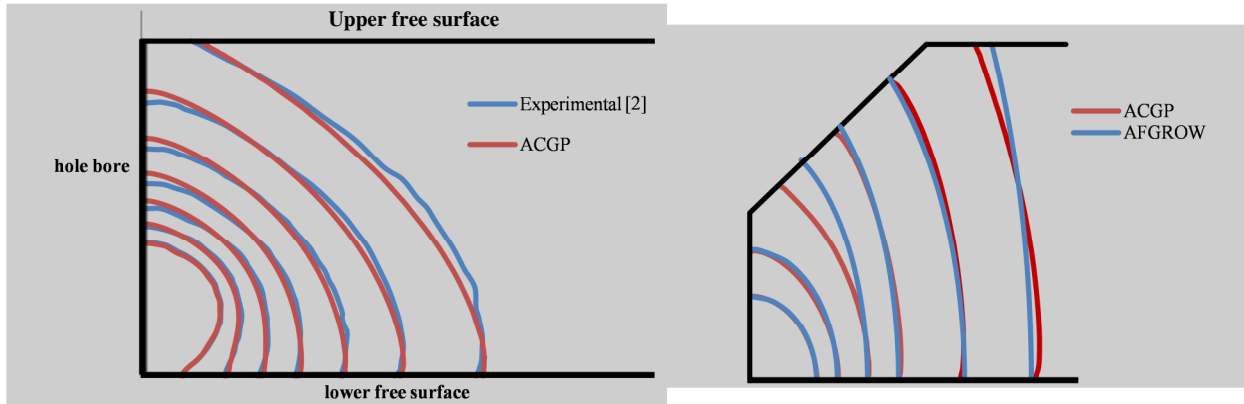


Figure 5.13 Comparison of experimental and ACGP crack front predictions for a corner crack at a straight hole (left image), b) AFGROW and ACGP predicted crack front shape for a corner crack from the bore of a countersunk hole (right image).

For corner cracks at straight holes and notches, the fatigue life predicted using the ACGP was longer than the predictions using AFGROW. This was due to AFGROW assuming an elliptical shape for the crack front, which resulted in higher ΔK values.

Future work includes exploring using this program as a basis for determining fatigue life for non-planar components such as spar caps.

5.6.1 REFERENCES

- [1] L. Alousis, "Numerical Predictions of Evolving Crack Front Geometry and Fatigue Life From Countersunk Holes in Thin Plates" M.A.Sc. Thesis, Royal Military College of Canada, October 2014.
- [2] R. Desnoyers and M. Liao, "Crack Growth Measurements Report on SENT Coupon J407-1E-2," LM-SMPL-2011-0202, 2011.

5.7 DEVELOPMENT OF A FATIGUE CRACK GROWTH RATE MATERIAL MODEL FOR 7249-T76511 ALUMINIUM ALLOY*

Y. Bombardier and M. Liao, NRC Aerospace

*Paper being presented at ICAF2015

The 7249-T76511 aluminium alloy is a relatively new alloy and is now entering service for new transport aircraft wings as a 'drop-in' replacement for existing 7075-T6511 aluminium alloy components. This alloy was optimized to maintain a high level of strength and fracture

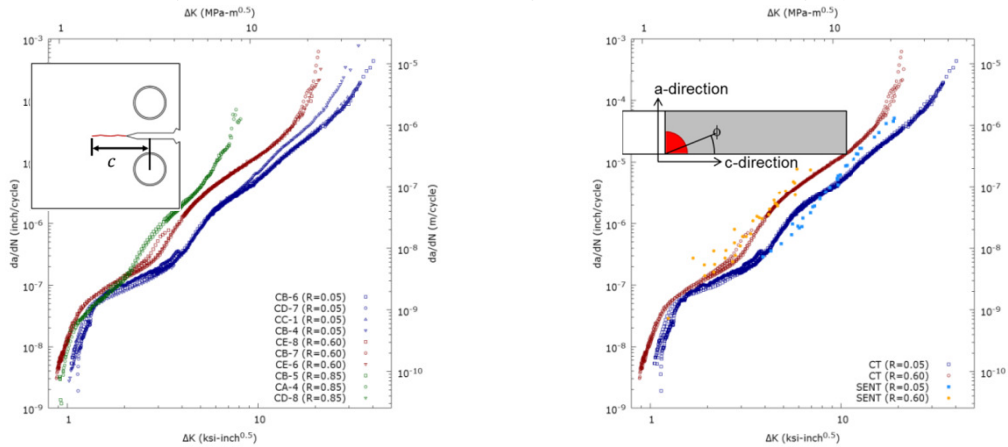
toughness, while improving its corrosion resistance over 7075-T6511. Despite the numerous advantages of using 7249-T76511 over 7075-T6511, no fatigue crack growth rate (FCGR) data could be found in publically available literature, which limits the ability to conduct fatigue life assessment of structures made of 7249-T76511. As it is expected that 7249-T76511 will be more commonly used for airframe components in the future, there is a need to obtain FCGR data and develop a model for this material to support current and future platforms.

FCGR tests were conducted for 7249-T76511 using C(T) and SENT specimens to characterize the fatigue crack growth properties of the material. C(T) test specimens were tested in laboratory air according to ASTM E 647 under three stress ratios: 0.05, 0.60, and 0.85. Overall, the variability of the FCGR test results obtained from the C(T) test specimens was small as shown in Figure 5.14a. The ACR method, used for the C(T) specimens, was found to reduce the effect of load history in the threshold regime when the initial K_{max} exceed the initial FCGR recommended in ASTM E 647. C(T) FCGR tests were also conducted in a 3.5% sodium chloride (NaCl) solution to quantify the effect of a corrosive environment on the FCGR. However, it was found that the cells used to contain the corrosive solution around the notch may have influenced the FCGR results and a new test method would be required to provide accurate FCGR results in the threshold regime. SENT tests were performed to determine the FCGR of small cracks naturally nucleating from a notch. As shown in Figure 5.14b, the FCGR obtained from these tests were in good agreement with the long-crack FCGR results obtained using the C(T) specimens. However, no FCGR results could be obtained in the stress intensity factor threshold regime using the SENT specimens as the marker bands corresponding to the smallest crack sizes could not be found from fractography.

Using the results from the steady-state FCGR tests, two FCGR material models were developed. A tabular look-up model was first developed to interpolate and extrapolate the FCGR data for different stress ratios. This model was combined with a load interaction model to consider crack retardation effects for crack growth simulations under variable amplitude loadings. The load interaction models were calibrated using a subset of variable amplitude loading test data and verified with other test data. Overall, the selected load interaction parameters provided acceptable results, but there is a strong possibility that these parameters may not be suitable for other loading spectra. Unlike the tabular look-up model with load interaction models, the FASTRAN model presented in this paper was developed solely based on the steady-state FCGR data. Comparison between the crack growth analysis results and experimental results are summarized in Figure 5.15. Although not finalized yet, the current FASTRAN material model developed by NRC seems promising due to the facts that it was not developed by tuning its parameters to fit variable amplitude spectrum results and that it could simulate the effects of spike overloads on the FCGR.

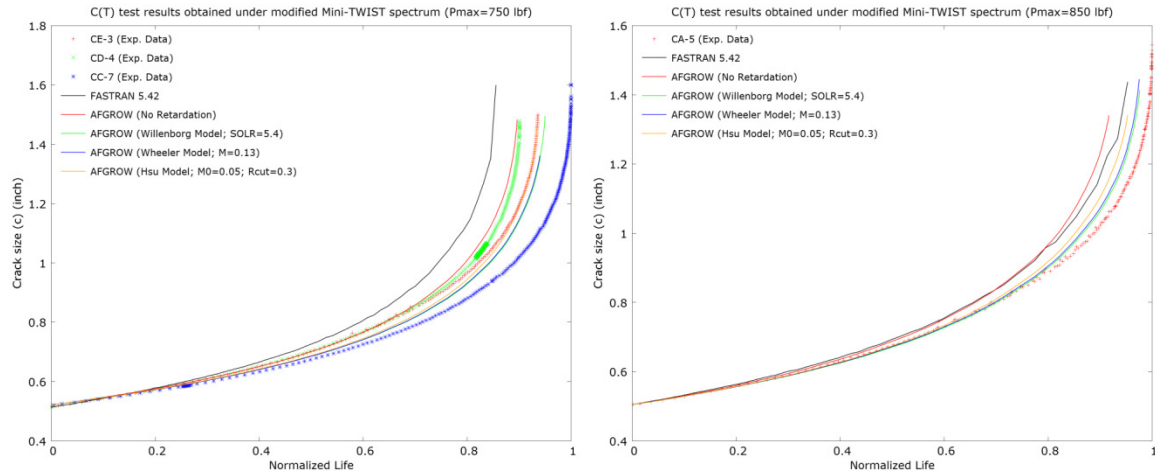
The FCGR material models developed using the steady-state FCGR results need to be improved and fine-tuned using additional steady state FCGR data (e.g. negative stress ratio, effect of thickness, other coupon geometries) to improve the accuracy of the fatigue life calculations. Additional variable amplitude loading fatigue test data is also required to gain confidence on the accuracy of the proposed material model and identify its limits.

Review of Canadian Aeronautical Fatigue and Structural Integrity Work 2013-2015

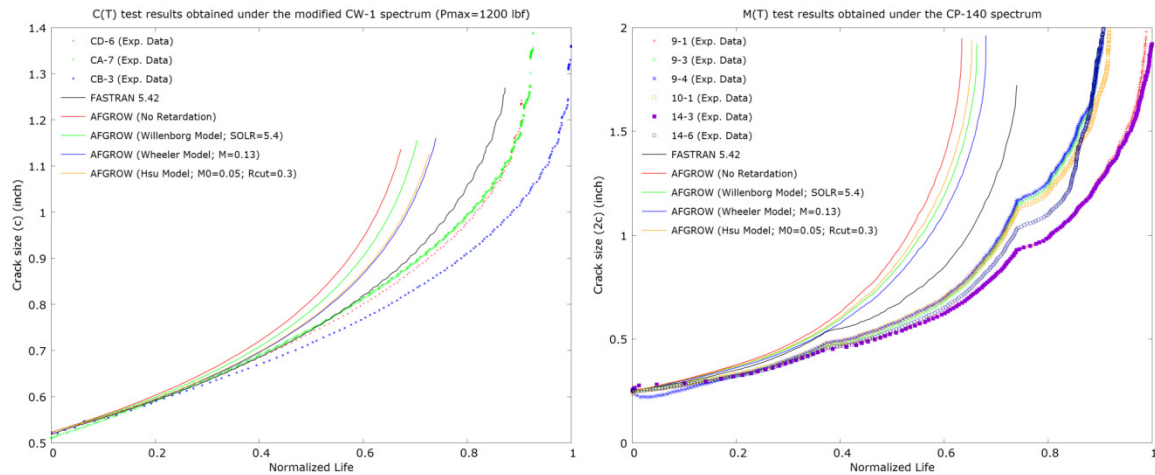


a) Long crack FCGR results obtained using C(T) specimens b) Comparison between long crack (C(T)) and short crack (SENT) FCGR results

Figure 5.14 7249-T76511 fatigue crack growth rate experimental data and fitted curves for laboratory environment



a) Fatigue life prediction for the modified Mini-TWIST spectrum (maximum load of 750 lbf) b) Fatigue life prediction for the modified Mini-TWIST spectrum (maximum load of 850 lbf)



c) Fatigue life prediction for the CC-130 test spectrum (maximum load of 1200 lbf) d) Fatigue life prediction for the CP-140 test spectrum

Figure 5.15: Fatigue crack growth predictions

5.8 PREDICTIVE MODELING FOR FOUR-POINT BENDING OF THIN CARBON-EPOXY LAMINATES

C. Marsden, Royal Military College of Canada

Aerospace structural design makes extensive use of thin carbon fibre reinforced plastics (CFRP) laminates in applications such as skins, stiffeners and frames. Flexural tests induce complex stress fields and may therefore be good candidates for the efficient evaluation of the behaviour of thin laminates under static and fatigue loads. Standard methods for static flexural testing of carbon-reinforced epoxy composites are outlined in ASTM D6272-10 Standard Test Method for Flexural Properties of Unreinforced and Reinforced Plastics and Electrical Insulating Materials by Four-Point Bending, and ISO 14125: 1998 Fibre-reinforced plastic. If flexural tests are to be used as an effective design tool to characterize carbon-epoxy laminate behaviour in terms of flexural modulus, ultimate strength, buckling instability and fatigue performance, the effects of test fixture geometry, coupon size, ply angle and stacking sequence on the results of the test need to be accounted for in the analysis of test data.

Based on experimental test results for fatigue tests in four-point bending on thin carbon-epoxy laminates, this project uses finite element modeling to investigate the effects of test fixture design, coupon geometry, friction in the test apparatus, and coupon thickness on the experimentally determined value of flexural stiffness. For fatigue testing, the use of load introduction tabs as shown in Figure 5.16a is necessary to prevent coupon damage as shown in Figure 5.16b.

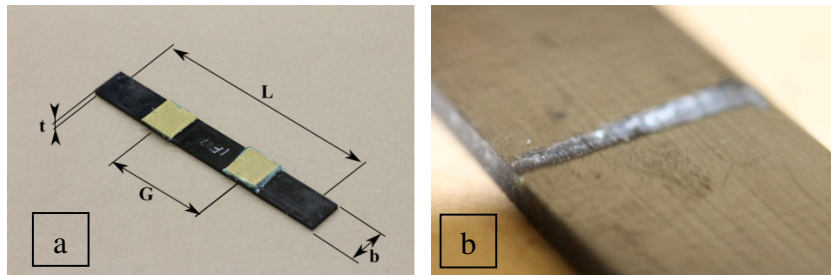


Figure 5.16 a) four-point bend fatigue coupon with Kevlar load introduction tabs, b) fatigue coupon damaged at load introduction point after 10,000 cycles

Friction between the loading noses and the load introduction tabs introduces an “apparent hysteresis” effect as shown in Figure 5.17a, where the solid line is the force displacement curve for one cycle with no friction and the dotted curve demonstrates the effect of friction on the force displacement cycle. Figure 5.17b shows the finite element model with and without friction for the same test. The finite element model can effectively predict the effect of differing coefficients of friction on the slope of the load-deflection curve and the predicted bending stiffness.

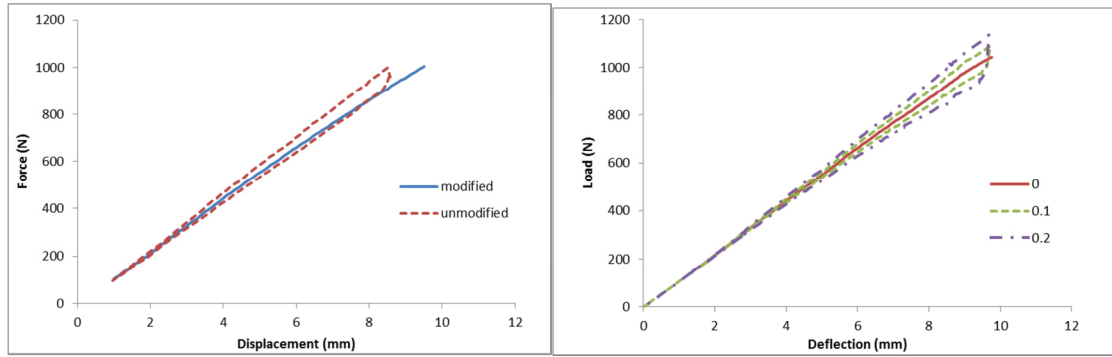


Figure 5.17 a) experimental results with (dashed line) and without (solid line) friction, b) finite element simulations of the experimental setup with and without friction

The finite element model can effectively predict the expected differences in the slope of the load-deflection curve and apparent bending stiffness due to variations in coupon thickness. Figure 5.18 shows experimental and numerical results for two 16-ply cross-ply coupons of the same nominal thickness where the actual measured thickness difference was 0.17 mm.

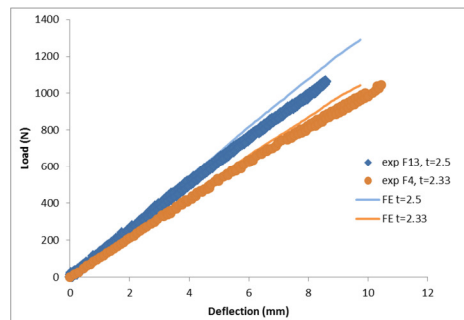


Figure 5.18 Experimental and finite element results showing the effect of coupon thickness on measured bending stiffness of 16-ply, cross-ply laminates

The model has been extended to investigate the effect of angle-ply lay-ups on the assumption of uniformly distributed maximum axial fibre stress between the loading noses and uniform shear outboard of the loading noses for four-point bending tests. Figure 5.19a compares shear stress distributions along the coupon length for 0-degree (uni-directional) and 20-degree (angle ply) laminates. Figure 5.19b shows the asymmetrical distribution of stresses across the width of the four-point bend coupon for the 20-degree angle ply laminate.

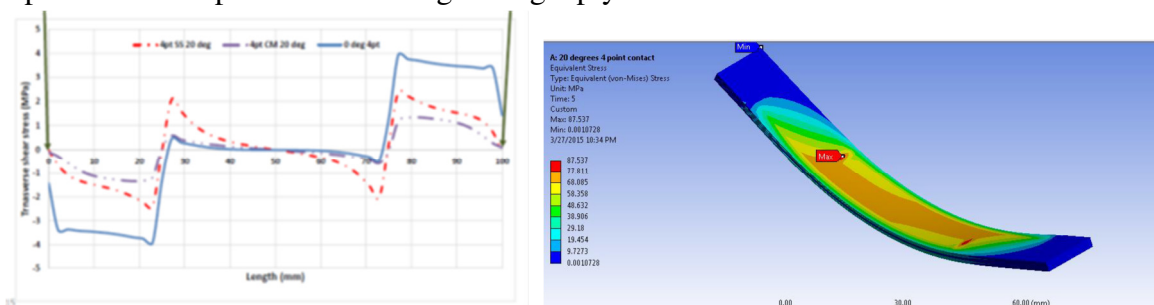


Figure 5.19 a) Out-of-plane shear distribution along the length of uni-directional (solid line) and 20-degree angle ply coupons under four-point bending; b) asymmetrical stress distribution for 20-degree angle-ply laminate under four-point bending

6.0 USAGE AND STRUCTURAL HEALTH MONITORING

6.1 DATA REDUCTION OF FLIGHT TEST AND FEM DATA SETS AND APPLICATION TO FATIGUE LOAD SPECTRA DEVELOPMENT

Ould Brahim Nazim and Lapalme Maxime, Bell Helicopter Textron Canada

Flight test data gathered using an instrumented production representative test aircraft is often seen as the most accurate and reliable method of creating a fatigue load envelope for airframe components. These tests often involve dozens of instrumented channels, capturing thousands of data points per flight, and hundreds of flight test conditions. This results in a very large multidimensional (multichannel) dataset, which can be impossible to parse for the most critical component and the most severe loading conditions.

The traditional approach has been to select one (or at most 2) independent load channels at a time and find the maximum and minimum loads. This approach is completely blind to the effect of combined loading (fundamentally multidimensional) and can result in a very liberal, one dimensional view of the load envelope. In the end, one has to rely on engineering judgment to find the approximate peak load conditions for any given component. There are two roadblocks to using a true multidimensional approach to select the load envelope:

1. Visualizing a multidimensional dataset in a meaningful way is daunting, and in many cases impossible.
2. The number of load combinations which define the fatigue envelope becomes too large. Stress and fatigue analysis of components becomes difficult via traditional approaches.

The proposed solution aims to remedy both issues with a single unified approach. Using convex hulls, it is possible to extract and simplify n-dimensional load envelopes in a way which ensures the peaks are maintained. This results in a greatly reduced dataset (beyond 99% reduction in our case studies). A large multidimensional load envelope, once reduced may still be too large to quickly assess the stress and fatigue life of airframe components using traditional approaches, including Finite Element (FE). When using linear FE models, the convex hull approach can be used to reduce the set of potentially critical elements. With these two large datasets reduced to a more manageable size, it becomes easy to assess the full effect of the entire fatigue envelope on any section of the aircraft. Furthermore, due to the nature of convex hulls, it is guaranteed that the highest and lowest load conditions are contained for any given component; this creates a repeatable, predictable method for selecting fatigue test load conditions from flight test datasets.

Bell Helicopter Model 429 aft fuse and tailboom composite structures were used as a test case for this approach. By extracting only critical loading conditions, the flight test dataset is reduced from millions of points to thousands of points; thus enabling analysis capabilities which would have otherwise been too time consuming.

Using this reduced data, derived load conditions were applied to an FE model representing the model 429 tailboom and aft fuse structure to assess fatigue damage. A convex hull approach is applied to reduce the scale of the model and results allowing the identification of critical

composite plies and loading directions, using a ply by ply analysis method. Using the critical elements and the reduced flight data provided an effective way of determining the strains at critical regions. This simplified model correlated perfectly with the original model, with both models showing the same maximum and minimum stresses and load conditions for all components. The load conditions found to be the most severe were not inherently intuitive when looking at the flight test datasets. They represented a critical combination of flight loads which did not correspond with the highest load found in any given channel.

This dataset was further leveraged, notably to derive representative load conditions for composite repair patch testing. Loading R-ratios are critical in composite testing and allowable determination. These ratios have a strong impact on fatigue life of composite materials. Analysis of the Bell model 429 tailboom and aft fuse structure was required to derive the most appropriate loading ratios under critical flight loads for testing.

Analysis of the oscillatory strain distribution on reduced datasets permitted the identification of regions in which loading was both important in amplitude and presented the most detrimental ratios of compressive/tensile for the composite material in use. Correlation with experimental fatigue testing of Bell model 429 tailboom showed that the critical regions identified with the proposed methodology fully matched the damage observed on the experimental specimen.

The convex hull paradigm represents a powerful tool for analysis of linear sets, and when applied to structural and fatigue engineering problems, it can provide a novel and intuitive way of analyzing complex multidimensional data. Applications of this methodology permitted a timely and effective resolution of otherwise very complex and time consuming problems while ensuring the relevancy of results.

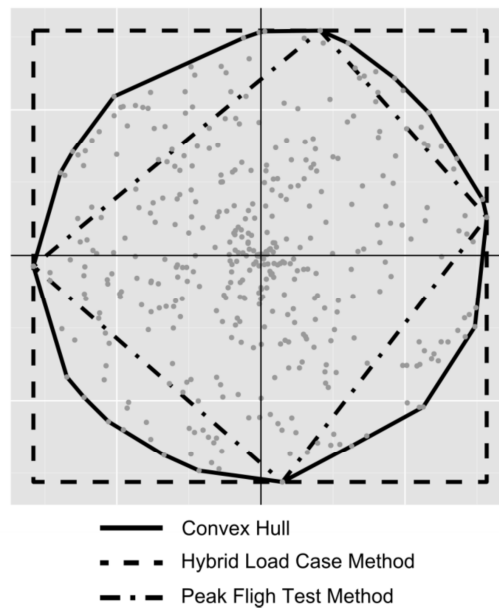


Figure 6.1 Two dimensional representations of fatigue load envelope extraction methods

6.2 ENVIRONMENTAL CONDITIONING FOR STRUCTURAL HEALTH MONITORING SYSTEM RELIABILITY*

D. Backman and S. Pant, NRC Aerospace

*Paper being presented at ICAF2015

As part of assessing and validating different SHM systems, the National Research Council Canada (NRC) has developed several SHM test platforms ranging from a simple cantilever beam to a wing-box structure. In this ongoing study the wing box structure similar to the complexity of the inner structure found in the CF-18 outer wing with fastened ribs, spars and skins was used to create representative hidden in-service fatigue damage of specific shape, size, and location as shown in Figure 6.2.

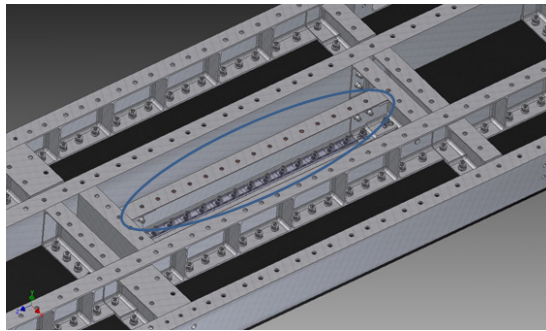


Figure 6.2 Internal rendering of the wing box showing the C-Channel where the hidden crack is located

In order to test various SHM sensor technologies under representative environmental conditions, the wing box was modified for temperature and pressure loadings. For temperature loading, the chamber could be heated using electric heaters and cooled using liquid nitrogen as shown in Figure 6.3.

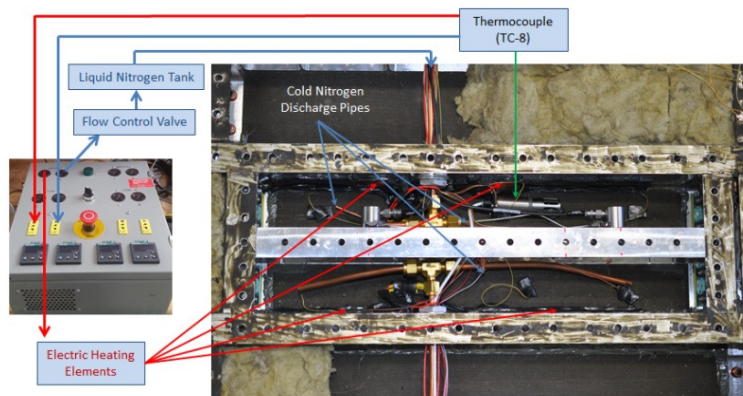


Figure 6.3 Setup of temperature loading

In conjunction with the temperature loading, pressure and humidity could also be changed within the test chamber for which the setup is shown in Figure 6.4.

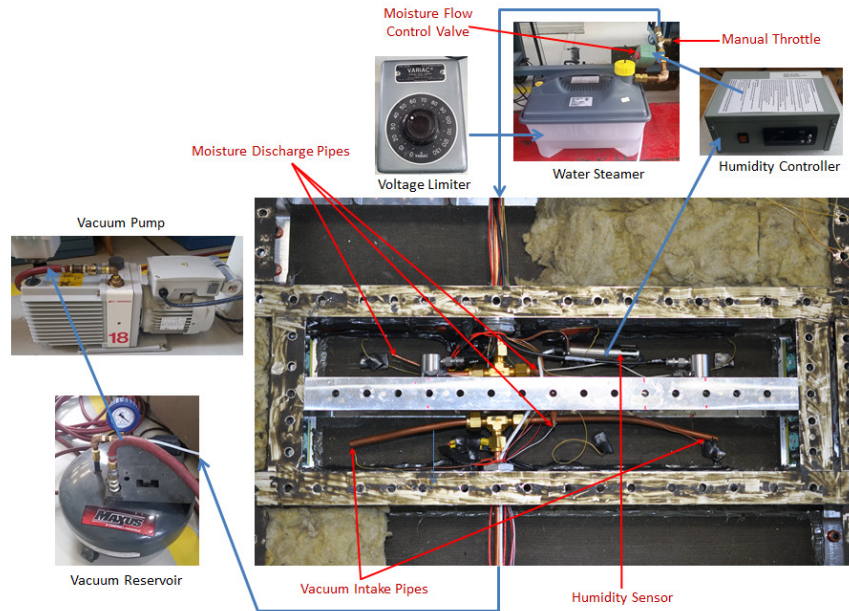


Figure 6.4 Setup for pressure and humidity

The ability to apply a combination of temperature, humidity, pressure, and fatigue load in a controlled environment is beneficial to economically testing the reliability of SHM systems under more realistic flight conditions as would be experienced on an aircraft.

6.3 LOW COST ACOUSTIC EMISSION SYSTEM FOR CRACK DETECTION IN STRUCTURAL HEALTH MONITORING TEST PLATFORM

S. Pant and D. Backman, NRC Aerospace

As part of a Defence Research and Development (DRDC) sponsored project on Structural Health Monitoring (SHM) reliability, a low cost, highly flexible Acoustic Emission (AE) system has been developed in-house. Acoustic Emission (AE) is a passive non-destructive evaluation (NDE) technology able to capture the acoustic signature of various crack growth and damage mechanisms in real time. The early detection of damage can be helpful in scheduling maintenance, predicting remaining life, and improve safety of the monitored components.

A validation experiment was recently completed in which NRC's in-house Acoustic Emission (AE) system was compared against visual inspection, Acoustic-Ultrasonic (AU), and Crack Indicator Sensor (KIS) Technology to determine its ability to detect crack growth. For this experiment all four technologies were used to monitor the fatigue crack growth in a complex C-Channel type structure made from aluminum (7075-T651). The removable C-Channel structure is a key component of the SHM reliability platform as it allows for the introduction of a specific type and location of damage that can be further grown in the SHM reliability platform subjected to fatigue loads. To generate the initial or seed crack in the C-Channel, it was loaded in tension-tension fatigue at 2 Hz with a max load of 11 kN (2500 lbf) and a load ratio of 0.01 as shown in Figure 6.5.

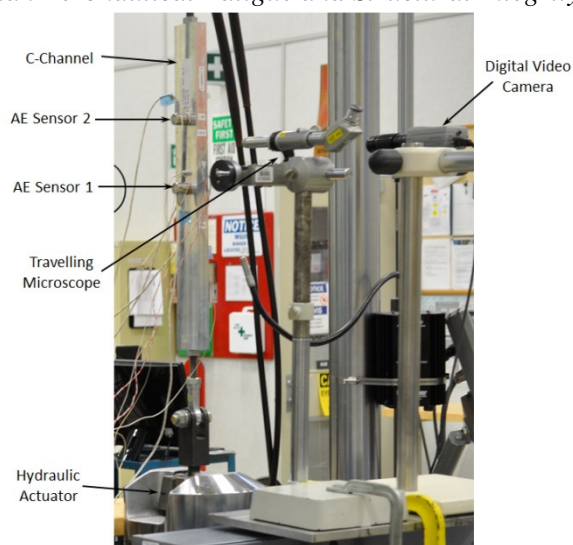


Figure 6.5 Fatigue crack test setup of C-Channel structure

The results of this experiment showed that NRC's in-house AE equipment was able to detect crack formation from a notch starting at 30K cycles, approximately 15K cycles before any other method including visual inspection through optical microscope. The AE system continued to register "hits" during the crack growth regime until the crack reached the desired final length of 2.54 mm.

6.4 KRACK INDICATOR SENSOR (KIS) TECHNOLOGY DEVELOPMENT – STRUCTURAL CRACK DETECTION & MONITORING

T. Benak and N. Bellinger, NRC Aerospace

There is a need for in-flight damage detection systems onboard aircraft structures that will provide timely and reliable warnings in the event of damage development in aerospace structures. A system has been prototype developed at NRC / Aerospace, that uses the Krack Indicator Sensor (KIS) Technology to detect and monitor fatigue cracks metal airframe structures, Figure 6.6. This KIS Technique provides a high degree of operator's confidence for fatigue crack detection (reliability) and subsequent fatigue crack length measurement (accuracy).

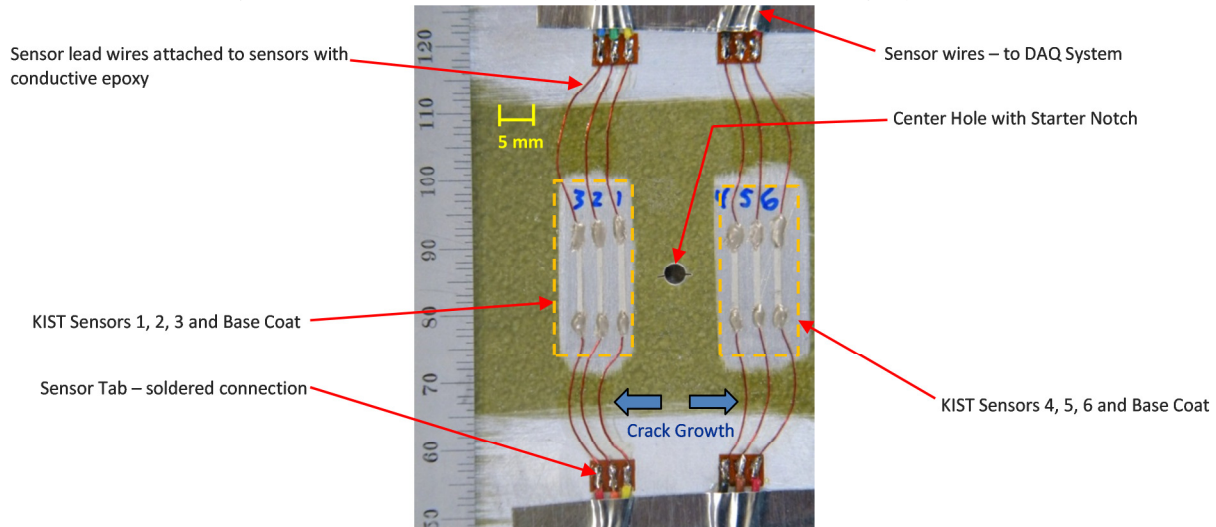


Figure 6.6 NRC Test Coupon during Prototype Development with KIS Technology System

The KIS Technology can be applied on aluminum material substrate for fatigue crack detection and/or monitoring. Fatigue cracks in the substrate material will allow for the sensor base coat to crack in a direct relationship. The conductive painted sensor will also break as the crack grows through the base coat and substrate material. Once the sensor is completely broken, the System trigger will be activated. See Figure 6.7 and 6.8.

Laboratory ambient conditions tests on aluminum sheet coupons have trialled over 120 sensors with a 100% reliability (sensor break indicating a crack in the substrate material) and with 90% accuracy (DAQ system trigger within +0.25mm tolerance), Figure 6.9. The KIS Technology has been successfully tested in laboratory ambient conditions at +4500 μ strain (typical fighter aircraft design load strain: +5000 μ strain and for cargo aircraft: +2000 μ strain).

The KIS Technology system has been proven to be (at room temperature ambient conditions) an extremely reliable system for the detection and monitoring of fatigue crack growth in aluminum structures, (Figure 6.10)

The advantages of the KIS Technology system are:

- [1] The sensors can be customized for the applicable area of concern.
- [2] The System process is easy to apply to the structure and with minimal training.
- [3] The fatigue crack growth in the substrate can be visually monitored if desired (clear base coat).

This technique has at this time, been applied only to room temperature aluminum sheet test coupons. On-going test efforts will investigate the accuracy and reliability of the KIS Technology system in hot / wet and cold test temperatures and humidity conditions and on various other substrate materials (steel, titanium, composites).

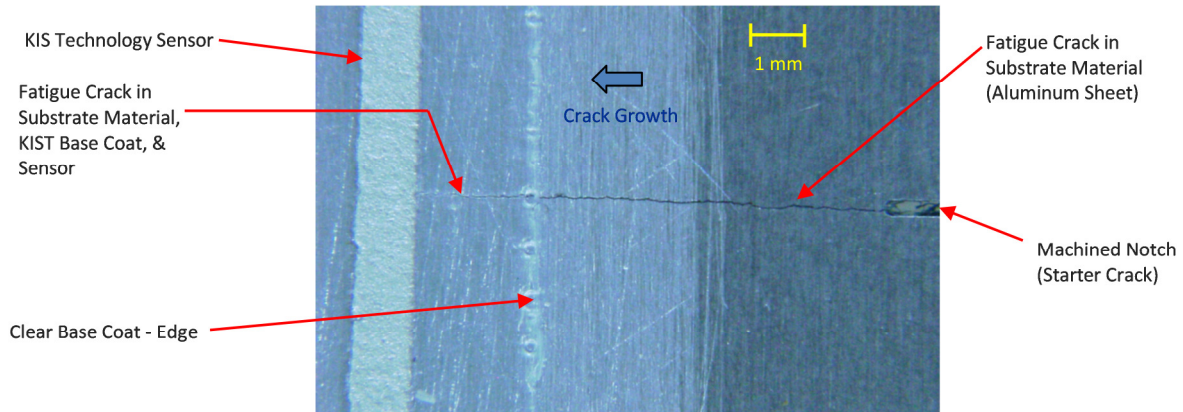


Figure 6.7 KIST System – Sensor at “Failure” to signal DAQ System Trigger (Sensor RELIABILITY)

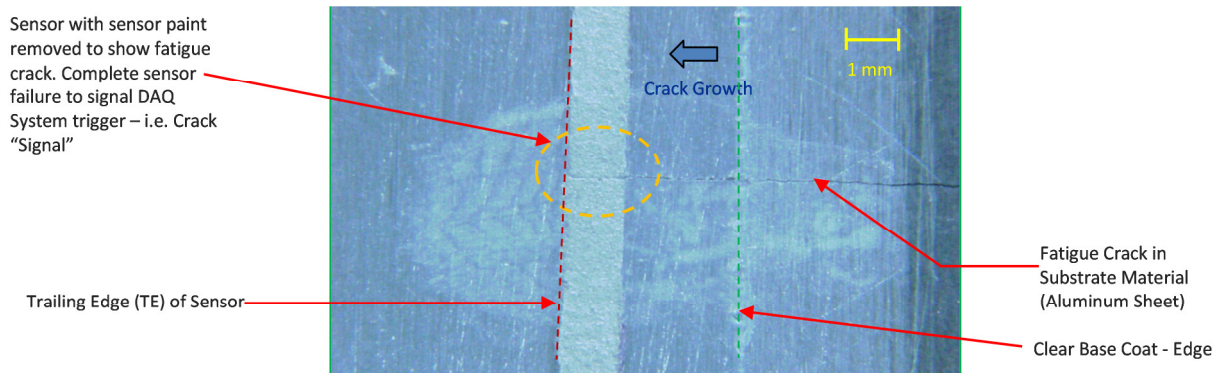


Figure 6.8 KIST System – Sensor at “Failure” – Sensor paint removed to show crack in sensor (Sensor RELIABILITY)

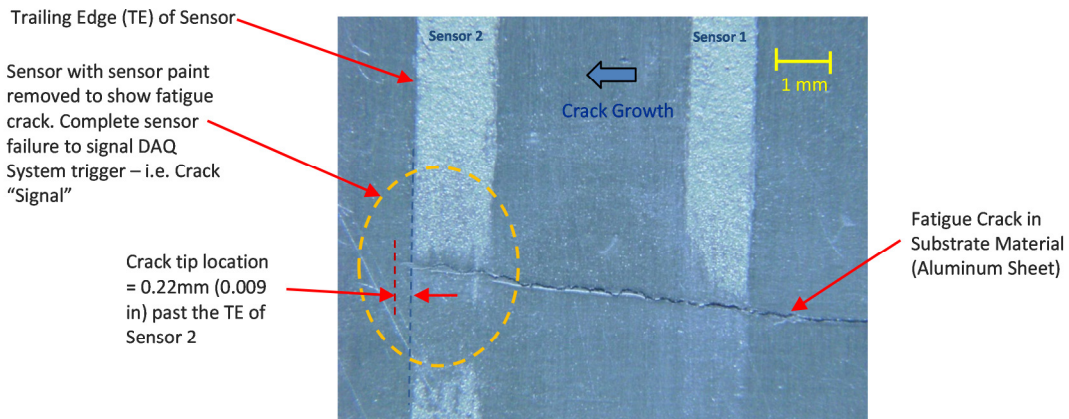


Figure 6.9 KIST System – Sensor No. 2 at “Failure” to signal DAQ System Trigger (Sensor ACCURACY)

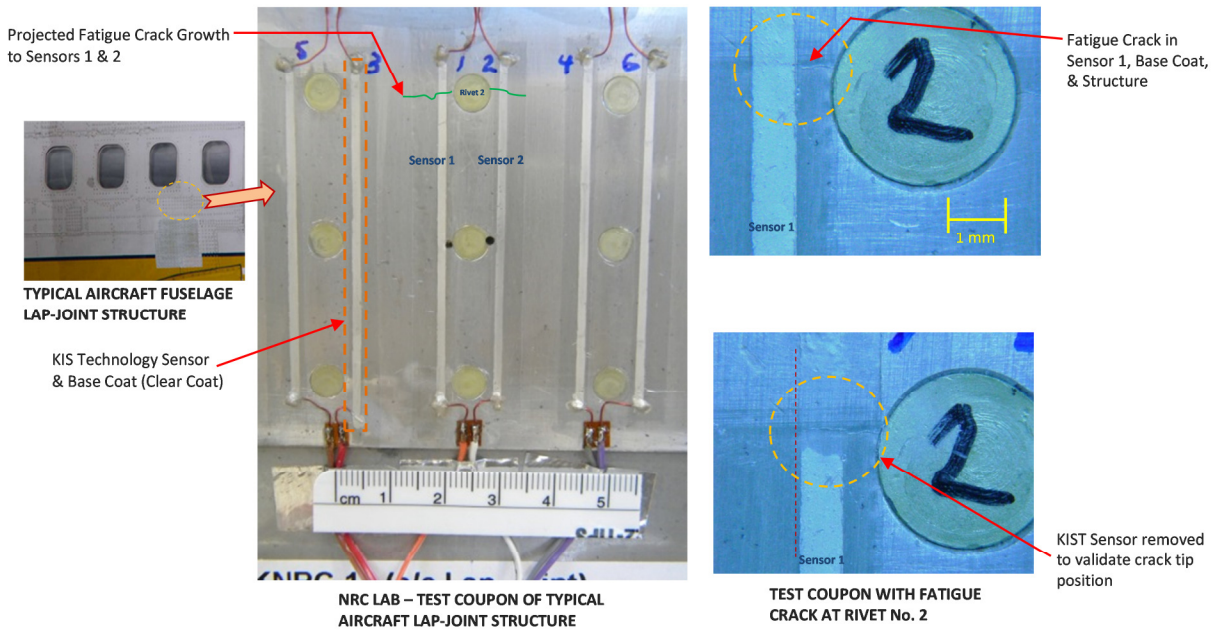


Figure 6.10 Typical Aircraft Lap-Joint Structure with KIS Technology System for Fatigue Crack Detection / Monitoring

6.5 HELICOPTER LOAD AND USAGE MONITORING: RESEARCH ACTIVITIES 2013-2015

C. Cheung, NRC Aerospace

Helicopter Load Monitoring

Since operational requirements have significantly expanded the role of military helicopter fleets resulting in helicopters often flying missions beyond the design usage spectrum, there is a need to monitor individual aircraft usage and more accurately determine the life of critical components to ensure flight safety and optimal aircraft usage. One of the key elements of tracking individual aircraft usage and calculating component retirement times is accurate determination of the component loads. Indirect methods to estimate loads on these components is a practical alternative to costly and maintenance-intensive measurement systems. Computational methods of estimating component loads and fatigue damage accumulation based on existing aircraft sensor data, such as flight state and control system parameters, have been in development at NRC over several years. The approach implements a number of computational intelligence methods and statistical techniques in exploring the data and building models to estimate the load signal in the component (Figure 6.11). Based on this estimated load signal, fatigue analysis is carried out including calculating the resulting fatigue damage accumulation and/or load exceedance curves (Figure 6.12).

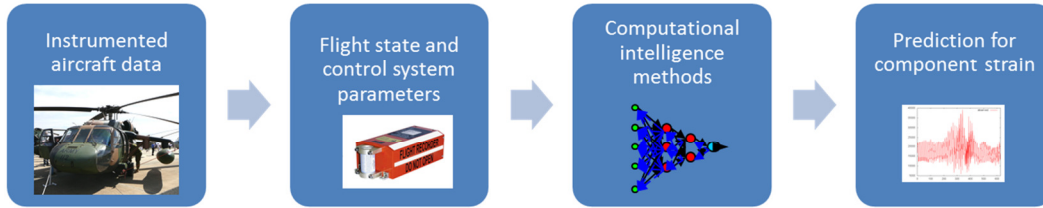


Figure 6.11 Component load signal prediction from flight state and control system parameters

Over the past 2 years, NRC's efforts have been focused on improving the methodology for load signal estimation to provide more accurate and correlated results, implementing the fatigue life analysis into the methodology, and validating the approach on other data sets. The results obtained thus far have shown tremendous potential for accurate and consistent estimates not only on the primary Black Hawk S-70A-9 dataset but also on initial efforts using a limited data set from the CH-146 Griffon. The work on the Black Hawk examined the main rotor pushrod axial load in 12 flight conditions as well as a general case, and the main rotor normal bending in 3 flight conditions; the Griffon work examined the main rotor yoke bending in 4 flight conditions and a general case. While the model primarily uses 'black-box' tools, i.e. artificial neural networks, significant effort has gone into exploring the input data to facilitate domain expert examination of the relationships between the flight state and control system parameters and component loads. In particular, a better understanding of the specific flight state parameters that are most relevant for particular loads in airframe and dynamic components of the helicopter can be obtained.

In addition to the progress made on the methodology for load and fatigue damage estimation, a helicopter experimental test rig was commissioned. This test rig consists of a helicopter tail boom (Bell 407) with 7 actuators installed and is intended to be used to apply representative load cases particular to helicopter structures (e.g. vibratory loads) and to explore structural health monitoring (SHM) technologies in conditions unique to helicopters (e.g. high-frequency loads).

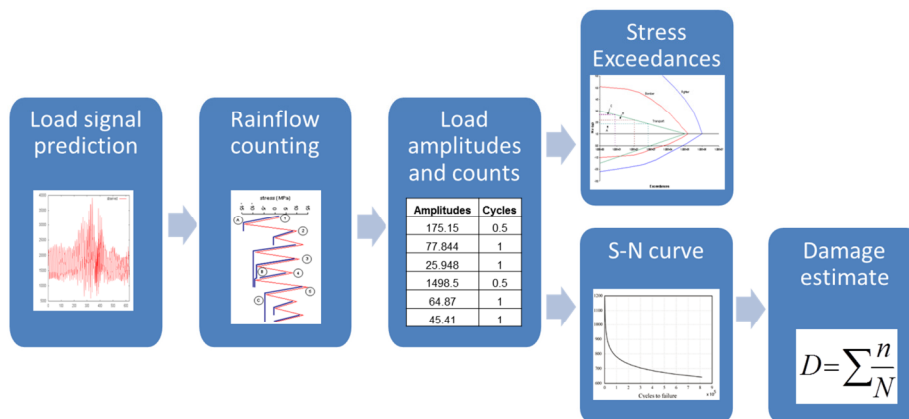


Figure 6.12: Fatigue life analysis

MEMS-IMU system for usage monitoring

As part of the fleet management and maintenance of military aircraft, basic usage spectrum (BUS) updates are performed regularly to capture fleet usage and operating details and compare

with the design usage. In the past, these BUS updates were performed using a combination of post flight checklists, pilot questionnaires and pilot interviews. As an alternative, NRC has developed a low-cost, standalone sensor system capable of detecting and recording flight manoeuvres. The data from this system could be used to provide a BUS update, but also could be used for aircraft usage and load monitoring, especially useful in aircraft that are not equipped with a health and usage monitoring system (HUMS) or a flight data recorder. The core of this sensor system is a microelectromechanical system inertial measurement unit (MEMS-IMU), composed of a GPS, pressure sensor, 3-axis accelerometer, gyroscope and magnetometer, and powered by a lithium ion battery. The system records accelerations, aircraft attitude rates, GPS position and velocities. With the aid of a power control unit, the system can operate for several weeks on a single battery charge. The components used for this system are commercial-off-the-shelf components, selected using an extensive evaluation. As part of this evaluation process, NRC developed a benchmarking protocol to verify sensor functionality, accuracy and reliability in different environments. A series of tests were carried out on individual components and the system as a whole to verify the operation of the components in different environments, such as cold-temperature, warm-temperature, and vibration. Static tests were also carried out to evaluate the natural noise and drift of the sensors, while dynamic testing was performed to assess sensor accuracy while undergoing a range of motion that may be expected from an aircraft.

Preliminary testing of this system has been carried out on NRC's experimental research helicopter (Bell 206) with further flight tests to take place later this year on the client's aircraft. Algorithms for flight condition recognition are currently in development using a number of computational intelligence techniques.

7.0 NON-DESTRUCTIVE EVALUATION

7.1 DEVELOPMENT OF INDUCTION HEATING THERMOGRAPHY

M. Genest, G. Li, and C. Mandache, NRC Aerospace

The induction thermography is a new method for the detection of cracks in electro conductive materials. In this method, the parts to be tested are heated up by an inductively generated current flow and the temperature profile generated thereby on the surface of the component is recorded with an infrared camera. This technique has been applied using periodic heating and phase sensitive detection for characterization of coating adhesion and using pulsed excitation for crack detection in turbine blades. New applications on steel components and carbon fibre reinforced polymers, and analytical and numerical modelling of the signal from cracks have also been reported.

This method can be applied for buried cracks where dye penetrant for closed cracks and near surface cracks cannot be used. Perpendicular cracks and slanted cracks can be detected in this way. If a coil is excited with an alternating current of high frequency, a current is induced at a certain depth position normal to the surface depending on the excitation frequency. The current lines run concentrically and are directed around disturbances, such as cracks. The current redirection around cracks leads to increased current density at crack tips and decreased current density at its flanks. The resulting local temperature change can be made visible with an appropriate thermographic camera.

The experimental setup for performing induction heating thermography has been developed and mounted on a gantry system that allows for automated scanning of components. Several coil shapes and sizes have been assessed.

7.2 DEVELOPMENT OF MODELLING CAPABILITIES FOR INDUCTION HEATING THERMOGRAPHY

G. Li, and M. Genest, NRC Aerospace

Induction heating is the process of heating an electrically conducting object by electromagnetic induction, where eddy currents are generated within the test piece and electrical resistance leads to Joule heating of the test piece. Unlike typical eddy current inspections, this technique is not sensitive to crack orientation or part geometry and have potentials to improve the inspection speed and ease the visualization of flaw detection in complex geometries. To efficiently apply this technique, development of the numerical capability is crucial to choose proper coil shape for generating practical heat distribution.

A numerical simulations and non-destructive evaluation (NDE) techniques for inductive heating of a 5 mm thick 7075 aluminum alloy panel were performed. A two-dimensional axis-symmetric finite element model was developed using COMSOL multiphysics software version 4. The panel was approximated by a disk with 0.5 mm diameter. In the NDE experimental testing, a 5 mm thick 7075-T6 aluminum alloy panel with dimension of 100x250 mm was heated using a copper coil with 3 loops in 50 mm external diameter. The alternative current used was 100 A with 200

kHz frequency. An infrared camera system was used to capture the panel temperature variation. The 2D axis-symmetric FE model meshed in two conditions and the temperature prediction profiles are shown in Figure 7.1. Results showed that the influence of the mesh condition on the temperature was limited, and good agreement was obtained between experimental results and the FE predictions. The impact of the inductor (coil) location, current level, and panel size on the temperature profile are also investigated using the FE model. The effort is to conduct parametric study to determine the parameters that significantly influence the temperature profile and for developing relevant 3D FE models and support the further development of induction thermography technique and procedures for damage detection.

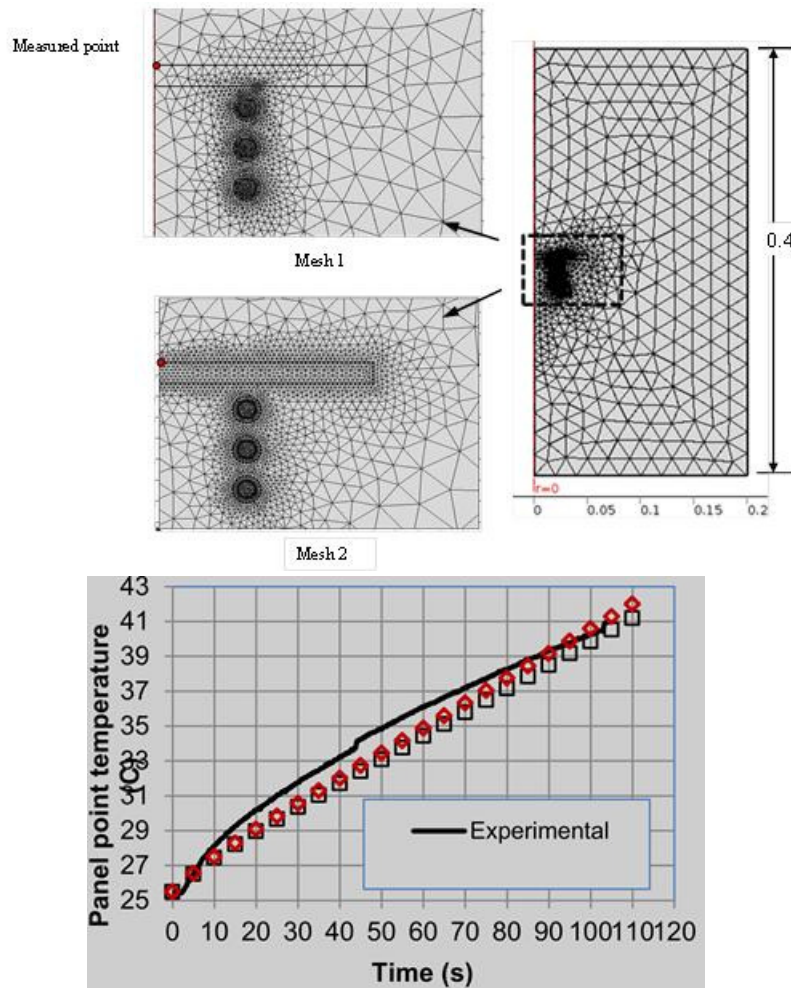


Figure 7.1 Induction heating of a 5 mm thick 7075 aluminum alloy panel: (a) two-dimensional axisymmetric FE models, and (b) temperature versus time profiles for a panel point obtained from experimental and numerical results.

7.3 COMPARATIVE ASSESSMENT OF NDT FOR THE INSPECTION OF CF18 OUTBOARD FORWARD RIB

M. Genest and M. Brothers, NRC Aerospace

Flight control surfaces (FCS) of some military aircraft are made of carbon fibre-reinforced polymer composite skins bonded onto aluminum honeycomb core. Over the years, FCS, such as

horizontal stabilators (HStab), are subject to impact damage, hail, and water ingress that can lead to disbonds. The HStab leading edge outboard forward rib of a Royal Canadian Air Force (RCAF) aircraft contains an area that is challenging for non-destructive inspection due to material stack up in that region. This caused current inspection procedure to lack the capability to detect some defects (misses) and a high number of false detection. Although currently treated as a non-inspectable area, it is desirable to have a reliable inspection technique for this area since it is subject to high dynamic loads and airflow. In this work, inspection results using pulsed thermography, bond testing and ultrasonic pulse echo are compared for inspecting different HStab outboard forward ribs. The inspection results revealed that both bond testing and pulsed thermography are capable of detecting disbonds in the outboard forward rib area of that aircraft HStab.

Non-destructive inspection results obtained using pulsed thermography, automated bond testing (BondMaster resonance mode) and automated ultrasound pulse-echo are compared in Figure 7.2. As can be seen, all three techniques detected the same disbonds. However the signal caused by the disbonds is easier to differentiate in the pulsed thermography and the bond testing results. The pulsed thermography inspection was the quickest to perform, taking only a few minutes, while the bond testing and ultrasonic pulse-echo took roughly 15 minutes per scan. In addition, due to the shape of the outboard forward rib area, it was sometime necessary to perform two different scans to cover the entire rib area with the ultrasonic and bond testing methods.

In addition, several infrared cameras were compared for use in the pulsed thermography inspection. It was demonstrated that, for the inspection of the outboard forward rib area, the thermal sensitivity of the IR camera is more important than the spatial resolution. Pulsed thermography inspection should use a camera that has a focal plan array of at least 320x240 pixels and a thermal sensitivity of 20mK. It was determined that pulsed thermography inspection results can be summarised by looking at only three images.

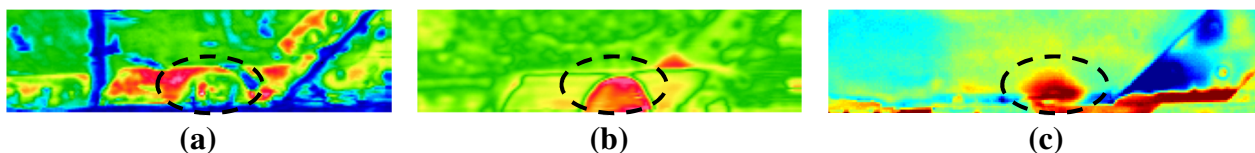


Figure 7.2 Inspection results from outboard forward rib area of an Hstab obtained by (a) ultrasound pulse-echo; (b) Bond testing; (c) pulsed thermography.

7.4 ASSESSMENT OF SHEAROGRAPHY FOR NDI OF COMPOSITE MATERIAL

M. Genest, NRC Aerospace

The NRC has been involved with shearography inspection of composite materials since 2008. Initially for the inspection of carbon fibre skin Nomex® core sandwich structures, and since then has assessed several other materials. In order to assess laser shearography capabilities and attempt to identify niche areas, a few parts were received from the Department of National Defence (DND) and inspected with the NRC laser shearography system.

If crushed core is an issue, shearography results have shown to be very sensitive to aluminum core damage and allow for detection of both crushed core in aluminum core sandwich parts and delam/disbond. However, it does not allow differentiating between the types of damage. For aluminum skin and core; among thermal, vacuum and vibration based shearography, thermal shearography provided the strongest image contrast and was the easiest to apply. Vacuum shearography when using portable shearography hood cannot always be applied due to surface features, presence of edges, holes in part, etc. that prevent forming a good seal with the part. Vibration based shearography seems to have too much variability based on the source location and pressure applied to make it practical for field implementation. It is also worth mentioning that NDT reference standards made for calibration of ultrasonic equipment may not be as useful and representative of real flaws for shearography methods and should be used with caution.

Findings show that shearography is a valuable NDT capability to have. However, the advantages over more traditional NDT methods and applicability are limited to some very specific cases. The main advantages were found when using vacuum shearography on composite skin Nomex® core sandwich structure or on rubber like material. Shearographic NDT is complex and requires a good knowledge of the structure being inspected and understanding of shearography measurements.

7.5 MODEL-ASSISTED PROBABILITY OF DETECTION ASSESSMENT FOR ENGINE COMPONENTS

C. Mandache and M. Khan, NRC Aerospace

Probability of Detection (POD) takes into account uncertainties occurring during the inspection and their response in terms of output variability. The POD curve, as determined based on empirical non-destructive investigations of parts is time, energy and cost demanding. Model-assisted POD (MAPOD) is an emerging concept. Its purpose is to reduce, but not eliminate the need for empirical inspections. In this way, significant time and capital resources necessary for empirical POD are considerably reduced. In the absence of fatigue cracks, MAPOD uses either simulated damage, such as electrically discharged machining (EDM) notches instead of fatigue cracks, or numerically-simulated signals. There are many situations for which MAPOD concepts are applicable, as for example changes in the inspection equipment parameters, and many others. The MAPOD approach is appropriate for *a-hat vs a* type of POD analysis. It finds an excellent application in the inspection of the engine disc serrations, since changes in the specimen size, as from one stage to another, or materials, as from one version of an engine to a newer one, are easily taken into consideration. In this way the number of specimens manufactured for the purpose of establishing a reliability measure for a specific NDI technique and procedure can be reduced.

In order to determine a POD curve, controlled laboratory inspections are normally employed. The inspected specimens may have:

- Naturally grown defects in real components.
- Artificial defects (*i.e.* EDM notches) in real components.

- Naturally grown defects in mock-up coupons.
- Artificial defects in mock-up coupons.

The targeted component of this project is the second stage turbine disc of the Rolls-Royce T56 engine. There are 18,000 units of this engine manufactured since 1954, for both military and civilian uses, while it was sold in nearly seventy countries. The T56 Series III engines power the CC-130 (Hercules) and CP-140 (Aurora) aircraft of the Royal Canadian Air Force. While these engines were designed and manufactured in 1980s, Rolls-Royce reduced the T56 turbine rotor life in 1997, based on new finite element models and low cycle fatigue data. However, many components have remaining life, beyond the manufacturer recommended safe-life limits. Stress and temperature effects accumulate at the serrated blade slots and microstructural damage lead to crack nucleation and propagation. Within their lifetime, engines are taken off the aircraft a number of times for maintenance, repair, and overhaul. Original Equipment Manufacturers (OEMs) are partnering with Maintenance, Repair and Overhaul (MROs) companies to build and maintain reliable and safe engines. NDI plays an important role in both, assuring the quality of newly made engines, integrity of in-service ones, while it drives their repair and re-design of subsequent versions. These engine components are designed for safe-life. In the case of legacy aircraft, it would result in significant cost savings if these engine parts were not discarded when there is significant residual life remaining and returned to service.

For this POD study, coupons replicating the lowest serration were manufactured from the same material as the T56 turbine disc material, *i.e.* waspaloy. The final shape and dimensions of the coupons were chosen in such a way that they will match those of the actual lowest serration of the turbine disc when two coupons are placed next to each other, as shown in 7.3.

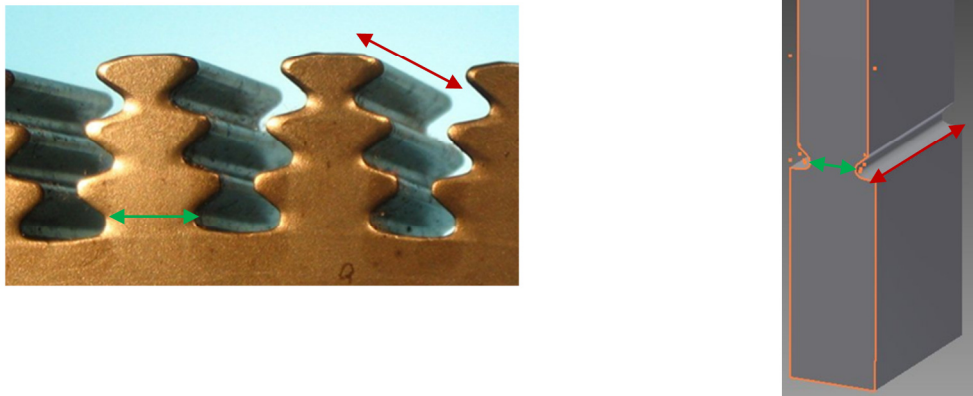


Figure 7.3 Picture of the turbine disc and schematic of the coupon replicating half of the lowest serration geometry. The width and length of the coupon are the same as in the real component

The possible crack locations were expected to be either in the centre or close to the edge of the coupon along the area indicated to have the highest stresses in Figure 7.4. For eddy current inspections the most challenging situation is when cracks are close to the edge of the serration and this is due to the influences of the edge effects on the signals.

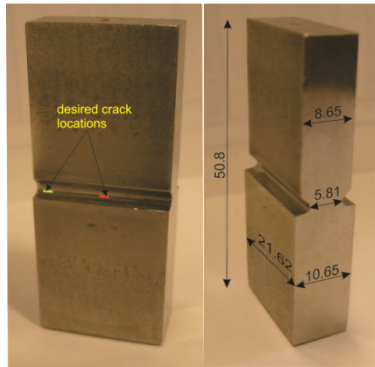


Figure 7.4 Coupons representing half of the serration on each side (dimensions given in millimeters)

This POD study in the ‘a-hat vs a’ type of analysis needs 40 defect-containing inspection sites and three times more (120) blank (with no defect) sites. The idea was to have the cracked coupons assembled with the blanks in configurations of 40 at a time: about 10 cracked coupons along with 30 blanks. Once these are inspected, the blanks will be re-used in the next configuration, with other cracked coupons different from the ones in the first set, and so on to a total of four configurations. All the blank coupons are already manufactured. An assembled configuration would look like the one in Figure 7.5.

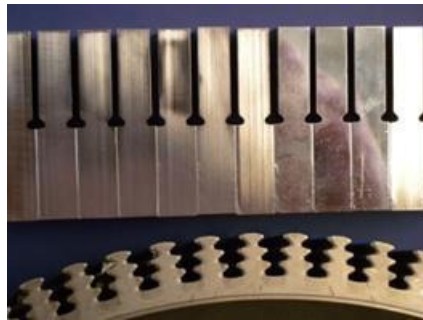


Figure 7.5 Desired coupon assembly to represent a series of lower serrations arranged linearly